Cardiovascular Diabetology

RESEARCH

Open Access

Adipsin improves diabetic hindlimb ischemia through SERPINE1 dependent angiogenesis

Xiaohua Zhang[1†], Mengyuan Jiang[1†], Xuebin Zhang[1†], Yixuan Zuo[1], Huanle Zhang[1], Tingting Zhang[2], Liyu Yang[1], Jie Lin[1], Yan Zhang[1], Xinchun Dai[1], Wen Ge[1], Chuang Sun[1], Fang Yang[3], Jiye Zhang[1], Yue Liu[1], Yangyang Wang[1], Huanhuan Qiang[1], Xiaojie Yang[1] and Dongdong Sun[1*]

Abstract

Background Adipsin (complement factor D, CFD), as the first described adipokine, is well-known for its regulatory effects in diabetic cardiovascular complications. However, its role in diabetic hind-limb ischemia was not clarified. This study aimed to evaluate the possible therapeutic effect of Adipsin in hind-limb ischemia in type 2 diabetic mice and to elucidate the molecular mechanisms involved.

Methods A high-fat diet and streptozotocin (HFD/STZ)-induced diabetic mouse model, and a transgenic mouse model with adipose tissue-specific overexpression of Adipsin (Adipsin-Tg) were employed. Hindlimb ischemia was established by femoral artery ligation, and blood flow recovery was monitored using Laser Doppler perfusion imaging. Molecular mechanisms underlying Adipsin-potentiated angiogenesis were examined using RNA sequencing and co-immunoprecipitation/mass spectrometry (Co-IP/MS) analyses.

Results Adipsin expression was upregulated in non-diabetic mice following HLI, while suppressed in diabetic mice, indicating its potential role in ischemic recovery which is impaired in diabetes. Adipsin-Tg mice exhibited significantly improved blood flow recovery, increased capillary density, and enhanced muscle regeneration in comparison with non-transgenic (NTg) diabetic mice. Adipsin facilitated proliferation, migration, and tube formation of human umbilical vein endothelial cells (HUVECs) under hyperglycemic and hypoxic conditions. Additionally, it enhanced phosphorylation of AKT, ERK, and eNOS pathways both in vivo and in vitro. RNA sequencing and co-immunoprecipitation/mass spectrometry (Co-IP/MS) analyses identified that Adipsin promoted angiogenesis by interacting with SERBP1, which disrupted the binding of SERBP1 to *SERPINE1* mRNA, resulting in reduced SERPINE1 expression and the subsequent activation of the VEGFR2 signaling cascade.

Conclusions Adipsin promotes angiogenesis and facilitates blood perfusion recovery in diabetic mice with HLI by downregulating SERPINE1 through interaction with SERBP1. These findings elucidate a novel therapeutic potential for Adipsin in the management of PAD in diabetic patients, highlighting its role in enhancing angiogenesis and tissue repair.

Keywords Diabetes, Hindlimb ischemia, Angiogenesis, Adipsin, Endothelial cells

†Xiaohua Zhang, Mengyuan Jiang and Xuebin Zhang have equally contributed to this work.

*Correspondence:
Dongdong Sun
wintersun3@fmmu.edu.cn

[1]Department of Cardiology, Xijing Hospital, Air Force Medical University, Xi'an, China
[2]Xijing 986 Hospital Department, Air Force Medical University, Xi'an, China
[3]Basic Medical Teaching Experiment Center, Basic Medical College, Air Force Medical University, Xi'an, China

Introduction

Type 2 diabetes mellitus (T2DM) is a chronic and complex metabolic disorder caused by impaired insulin secretion or reduced insulin sensitivity [1]. This condition poses a formidable global health crisis, with increasing incidence rates imposing substantial socioeconomic burdens on society [2]. Prolonged hyperglycemia in T2DM leads to a range of clinical complications associated with metabolic syndrome [2, 3]. One major complication is lower-extremity peripheral artery disease (PAD), which can result in leg ulcers and, in severe cases, necessitate amputations [4, 5]. Furthermore, individuals with both PAD and diabetes exhibit more severe arterial disease and poorer outcomes compared to their non-diabetic counterparts [6]. These conditions often lead to significant physical disability, reduced productivity, and profound emotional distress [4]. Current therapeutic strategies for managing PAD in diabetic patients often fail to achieve satisfactory results. Both revascularization techniques and pharmacotherapies are limited by the impaired angiogenic response to the typical diabetic milieu [7]. Therefore, there is a critical need for new therapeutic approaches that can enhance angiogenesis and improve perfusion in ischemic tissues in the context of diabetes.

Angiogenesis, the biological process by which new capillaries emerge from pre-existing blood vessels, is a vital physiological mechanism, particularly essential for wound healing and restoration of blood flow following injury [8]. This intricate process involves proliferation, migration, and differentiation of endothelial cells (ECs), orchestrated by a multitude of signaling molecules and pathways [9]. However, in diabetic state, endothelial cells exhibit diminished proliferation and migration, contributing minimally to new blood vessel formation [10]. Within the context of PAD, angiogenesis functions as a crucial compensatory mechanism for restoration of blood flow to ischemic regions [9]. However, in diabetic patients, the angiogenic response is markedly compromised, primarily due to disrupted endothelial function and angiogenic signaling inherent in the diabetic milieu. This compromised angiogenesis exacerbates ischemic conditions, facilitating the risk of non-healing ulcers and limb amputation [5, 6, 11].

Adipsin, also known as complement factor D (CFD), is an adipokine primarily secreted by adipose tissue [12, 13]. It is a crucial component of the alternative complement pathway to catalyze the synthesis of C3a, the active form of complement component 3 (C3), playing an instrumental role in innate immunity [14, 15]. Beyond its immunological functions, recent studies have indicated that Adipsin may play a key role in ischemia-reperfusion and sepsis [16, 17]. In addition, Lo and colleagues have reported that Adipsin preserves β cells by catalyzing C3a formation in diabetic mice. Studies have shown that a correlation between Adipsin concentrations and the susceptibility to diabetes onset in adults [18]. Our earlier work depicted that Adipsin exerts a cardioprotective effect in the context of diabetic cardiomyopathy by enhancing mitochondrial function and mitigating myocardial lipotoxicity and lipid accumulation [19]. Moreover, adipose tissues release exosomes enriched with Adipsin, which are subsequently internalized by cardiac microvascular endothelial cells (CMECs), thereby exerting its protective function on CMECs [10]. The modulatory potential of Adipsin for EC function suggests that it may hold significant promise for hindlimb ischemia and impaired angiogenesis in diabetic patients.

In this study, we examined the role of Adipsin in promoting blood flow recovery through a comprehensive approach, utilizing a diabetic mouse model with induced HLI and a transgenic mouse model engineered to overexpress Adipsin specifically in adipose tissues. The present study revealed that Adipsin facilitated the restoration of blood flow and promoted angiogenesis in diabetic HLI. Mechanistic studies indicated that Adipsin interacts with SERBP1, thereby disrupting the binding between SERBP1 and *SERPINE1* mRNA, leading to a reduction in SERPINE1 expression. In consequence, endothelial cell proliferation and tube formation are enhanced, to promote angiogenesis. These findings elucidate a novel role for Adipsin in the promotion of angiogenesis.

Materials and methods

Animal models

All experimental protocols detailed herein received approval from the Institutional Animal Care and Use Committee of the Air Force Medical University (Approval ID: 20220617). Adipose tissue-specific Adipsin transgenic mice (Adipsin-Tg) were generated by crossing conditional Rosa26 Adipsin knock-in homozygous ($Adipsin^{LSL/LSL}Tg$) mice with Adipoq-Cre mice. Both $Adipsin^{LSL/LSL}Tg$ and Adipoq-Cre mice were procured from the Shanghai Model Organisms Center, and genotypes were confirmed using PCR analysis. Eight-week-old C57BL/6J mice were obtained from the Animal Center of the Air Force Medical University (Xi'an, China). Male mice were used in all animal experiments. Mice were housed under a controlled light/dark cycle at 23 °C for 12 h with free access to water.

To establish an animal model of type 2 diabetes mellitus (T2DM), mice were administered a high-fat diet (5.24 kcal/g; 60% of calories from fat, 20% of calories from protein and 20% of calories from carbohydrates) (HFD; Research Diets, D12492, USA), followed by streptozotocin (STZ; 50 mg/kg, Sigma Aldrich, S0130, Germany) injection, per the protocol defined in previous literature [10]. Eight-week-old male C57BL6 Adipsin-Tg and NTg mice were subjected to either an HFD or a

normal diet (ND; Research Diets, D12450J, USA) for 16 weeks. After 15 weeks of dietary regimen, mice with glucose intolerance were intraperitoneally injected with STZ or an equivalent volume of citrate buffer for 5 consecutive days. One week after the final STZ injection, mice that did not fulfill the diagnostic criteria for diabetes were excluded from the experiments. Glucose tolerance test (GTT) was conducted to confirm hyperglycemia. Blood glucose levels were monitored using blood samples obtained from the tail vein, and only mice with blood glucose levels > 16.6 mmol/L were considered diabetic and used for experiments.

Immunofluorescence staining

Ischemic and control gastrocnemius muscles were harvested from the hind limbs of mice. The collected tissues were fixed in 4% paraformaldehyde (PFA), washed with phosphate-buffered saline (PBS), dehydrated, embedded in paraffin, and sectioned at a 10-μm thickness. Sections were permeabilized and blocked for 1 h at room temperature with blocking buffer (Beyotime, C0265, China), and 0.1% Triton X-100 in PBS. Thereafter, sections were incubated with respective primary antibodies at 4°C overnight. Following primary antibody incubation, tissue sections were exposed to appropriate fluorescently labeled secondary antibodies for 1 h in the dark at room temperature. Nuclei were counterstained with DAPI (Beyotime, C1006, China). For the quantification of capillary and arteriole density, sections stained with anti-CD31 and α-SMA were examined using a confocal microscope. The vessel densities were analyzed using the ImageJ software.

HUVECs were collected and fixed in 4% PFA for 10 min at room temperature. Thereafter, fixed cells were permeabilized with 0.1% Triton X-100 in PBS for 10 min and blocked in 1% BSA for 1 h at room temperature. Cells were stained with primary antibodies at overnight 4°C. Subsequently, cells were incubated with the appropriate fluorescent secondary antibody for 1 h at room temperature. Images were acquired using a Nikon Eclipse Ti microscope at 60× magnification. Images were analyzed using the ImageJ software. Specific details for antibody dilutions are provided in the Supplementary Materials (Supplementary Material 1: Table S3).

Hind limb ischemia (HLI) surgery and assessments

Eight-week-old Adipsin-Tg and NTg mice, with or without T2DM induction, were used in hindlimb ischemia (HLI) experiments, with the appropriate optimization methods [20]. In brief, animals were anesthetized using inhaled isoflurane (2.5-4% isoflurane in 100% oxygen at a flow rate of 1 L/min) and placed on a heated blanket to maintain body temperature. Left hind limbs were shaved, and a 5-mm incision was conducted in the left thigh. The femoral artery was ligated at proximal and distal sites with two suture knots, followed by dissection and excision of small branches between the ligatures. The skin incisions were then meticulously closed with 4−0 surgical sutures.

A PeriCam perfusion speckle imager (PSI) (Perimed, PeriCam PSI, Sweden) was employed to monitor hindlimb blood flow at 0, 3, 7, and 14 days post-femoral artery ligation (dpl). Perfusion data were quantitatively analyzed by comparing the average perfusion of the ligated limb to that of the non-ligated limb, to minimize data variability. Following the completion of the experiments, mice were euthanized to collect ischemic and non-ischemic gastrocnemius muscles for subsequent analyses.

Motor function was evaluated at 14 dpl using an established scoring system: 0-flexion of the plantar or toe in response to tail traction; 1-plantar flexion; 2-absence of dragging but without plantar flexion; 3-foot dragging [21].

Hematoxylin and eosin (H&E) staining

Excised tissues were fixed in 4% PFA and subsequently embedded in paraffin. The paraffin sections were cut to a thickness of 4 μm. Following sectioning, samples were deparaffinized and rehydrated through a series of graded ethanol washes. The sections underwent histological staining, being treated with hematoxylin for 3 min and eosin for 1 min. Presence of myocytes with centrally located nuclei, a hallmark of muscle regeneration, was employed as an indicator to evaluate the extent of limb injury and the treatment efficacy. Total number of myocytes exhibiting centrally located nuclei was quantified and expressed as a percentage of the overall myocyte count per field [22].

Matrigel plug assay

The Matrigel plug assay was executed as delineated with appropriate optimization. In brief, mice were anesthetized using isoflurane and subcutaneously administered 200 μL of reduced growth factor Matrigel (Corning Falcon, 356230, USA) containing 30 ng/mL VEGF (Peprotech, 450−32, USA) and 50 units of heparin (Pfizer, USA), which rapidly solidified at physiological temperatures to form a solid plug. Following an incubation period for 7 days, the Matrigel plugs were extracted, homogenized in 500 μL of cell lysis buffer, and subjected to centrifugation at × 6000 g for 60 min at 4 °C. Hemoglobin levels were subsequently quantified by absorbance at 400 nm using the Hemoglobin Colorimetric Assay Kit (Beyotime, P0381S, China). Plugs were harvested for comprehensive histological and immunofluorescence staining. Quantification of angiogenesis was performed using the ImageJ software.

Cell culture and treatment

HUVECs were procured from iCell Bioscience Inc. (Shanghai, China, iCell-h110) and cultured in endothelial cell medium (ECM) (iCell Bioscience, China) supplemented with 10% fetal bovine serum (FBS), 100 units/mL penicillin, and 100 mg/mL streptomycin. For the purposes of this study, cell cultures were incubated in a high-glucose medium (25 mM glucose) within a normoxic incubator (20% O_2, 5% CO_2, 37 °C, humidified atmosphere) or subjected to hypoxic conditions (1% O_2, 5% CO_2 in N_2) with 5 mM glucose for 12 h [23]. Following exposure to normoxic and hypoxic environments, cells underwent a series of functional assays, including cell viability assays, migration assays, tube formation assays, and fluorescence detection.

Gene intervention

To enhance Adipsin expression, HUVECs were transduced with an Adipsin-overexpressing adenovirus (Ad-Adipsin) or an empty adenovirus (Ad-Control) at varying multiplicities of infection (MOIs) in an FBS-free medium, once cells had reached 50–60% confluence. Following an 8-hour infection period, medium was replaced with fresh medium containing 10% FBS. Cells were subsequently harvested 48 h later for further examination [24].

To downregulate the expression of SERPINE1 or SERBP1, three siRNAs were synthesized by Tsingke Biotechnology Company (Beijing, China) (Supplementary Material 1: Table S1). For in vitro studies, HUVECs were transfected using Lipofectamine 2000 (Thermo Fisher Scientific, Michigan, USA), and the siRNA with the highest knockdown efficiency was selected for conversion into a shRNA sequence. For in vivo studies, adeno-associated virus-1 (AAV1) vectors were engineered to carry an ICAM2 (intercellular adhesion molecule 2) promoter, along with Serpine1 or Serbp1 shRNA, or control shRNA constructs. All viral vectors were designed and constructed by Tsingke Biotechnology Company (Beijing, China). The sequences of shRNA for *Serpine1* is 5′-GGCCGACTTCACAAGTCTTTC-3′. The sequences of shRNA for *Serbp1* is 5′-GCGCTTAAGAAAGAAGGAATA-3′. The viruses were injected into the gastrocnemius muscles of both legs of NTg or Adipsin-Tg male mice two weeks prior to the induction of HLI.

CCK-8 proliferation assay

The Cell Counting Kit-8 (CCK-8) assay was utilized to quantitatively evaluate viability of HUVECs. HUVECs subjected to the specified treatments were initially seeded into 96-well plates at an approximate density of 5×10^3 cells per well. Subsequently, 10 μL of CCK-8 reagent (InCellGene, IC-1519, China) was added, ensuring homogeneous distribution. The plates were then placed back into the incubator for an additional 2-hour. Absorbance was recorded at 450 nm using a microplate reader (Molecular Devices, SpectraMax M5, USA).

EdU incorporation assay

To evaluate proliferation of HUVECs, the BeyoClick™ EdU-594 Cell Proliferation Assay Kit (Beyotime, C0078S, China) was utilized following the manufacturer's protocol. Fluorescence imaging was conducted with an Olympus IX73 microscope, and subsequent image analysis was executed using the ImageJ software to precisely quantify proliferative indices.

Wound healing assay

The wound healing assay was utilized to assess migratory capacity of HUVECs. In brief, HUVECs were plated in 6-well culture dishes and were maintained until reaching approximately 90% confluence. Subsequently, a linear wound was inflicted using the tip of a 200-μL sterile pipette, followed by rinsing with PBS to eliminate dislodged cells. The cultures were then maintained in either serum-free or low-serum medium, and images of wound areas were captured at 0 and 12 h post-scratch. Quantitative analysis of cell migration was conducted employing the ImageJ software to evaluate the extent of cellular movement.

Transwell assay

For transwell assay, we employed 6.5-mm Transwell inserts featuring an 8-μm pore size (Corning, 3422, USA). HUVECs at a density of 2×10^4 cells per well were seeded into the upper chamber, while 600 μL of medium supplemented with 10% FBS was introduced into the lower chamber. After 24 h of incubation at 37°C, HUVECs that had migrated across the membrane were subsequently fixed with 4% paraformaldehyde for 15 min, stained with 0.1% crystal violet (Beyotime, C0121, China) for 10 min, and subjected to quantitative analysis using an Olympus microscope.

Tube formation assay

For tube formation assay, 96-well cell culture plates were coated with 50 μL of Matrigel (Corning Falcon, 356230, USA) per well and were subsequently incubated at 37°C for 30 min to ensure polymerization. HUVECs were resuspended in endothelial cell medium and seeded onto the Matrigel at a density of 3×10^4 cells per well. Development of capillary-like tube structures was then observed using an Olympus microscope. The total tube length and the meshed area were quantitatively assessed using the ImageJ software. For enhanced visualization, the vascular network was segmented using ImageJ.

RNA extraction and quantitative RT-PCR

Total RNA was extracted employing the RNAsimple Total RNA Kit (TIANGEN, DP419, China). The RNA concentration was determined using a NanoDrop 2000 spectrophotometer (Thermo Fisher Scientific, Michigan, USA). Reverse transcription of RNA to cDNA was carried out utilizing the PrimeScript RT reagent kit (Takara, RR036A, Japan). Quantitative real-time PCR (RT-qPCR) analysis was subsequently conducted using the CFX96 Real-Time System (Bio-Rad) with SYBR Premix Ex Taq II (TaKaRa, RR820A, Japan). Detailed primer sequences are provided in the Supplementary Material (Supplementary Material 1: Table S2).

Western blotting

Cells were lysed on ice using a RIPA lysis buffer containing PMSF, protease inhibitors, and phosphatase inhibitors. Concurrently, muscle tissues were homogenized using a homogenizer (TissueLyser LT, 85600, Germany) according to the manufacturer's instructions. The lysates were centrifuged at 12,000 rpm for 30 min at 4°C (HITACHI, CT15RE, Japan), and supernatants were collected for Western blotting analysis. Protein concentrations were determined using the BCA protein assay kit (Beyotime, P0010, China). Proteins were separated by sodium dodecyl sulfate-polyacrylamide gels (SDS-PAGE; ACE, ET12420LGel, China) and transferred onto polyvinylidene difluoride (PVDF) membranes (Millipore, MA, USA). Target proteins were incubated with specified primary antibodies overnight at 4°C, followed by incubation with appropriate secondary antibodies for 1 h at room temperature. Enhanced chemiluminescence (ECL) color bands were visualized using chemiluminescence technology. Densitometric analysis was conducted utilizing the ImageJ software. Details of primary antibodies are provided in Supplementary Material (Supplementary Material 1: Table S3).

Co-immunoprecipitation (Co-IP)

For preparation of HUVEC antigen samples, protein A/G immunoprecipitation magnetic beads (InCellGenE, IC-8110, China) were utilized. The magnetic beads were preprocessed and conjugated with anti-Adipsin and anti-SERBP1 antibodies, precipitated and eluted antigens, following the manufacturer's protocol. Subsequently, 20–50 μL of 1× loading buffer was added to the processed antigen samples. The mixture was thoroughly stirred and heated at 95°C for 5 min before undergoing a second round of magnetic separation. The supernatant was collected and transferred to a new Eppendorf tube. Following centrifugation at 13,000 g for 10 min at room temperature, the supernatant was collected for subsequent analysis [19].

Immunoprecipitation and mass spectrometry (MS) analysis

Initially, HUVECs were exposed to Adenovirus expressing Adipsin (Ad-Adipsin) under hyperglycemic hypoxic conditions. Following this treatment, a co-immunoprecipitation (Co-IP) assay was conducted targeting Adipsin. Proteins that were immunoprecipitated were subsequently subjected to MS analysis by Q-Exactive HF-X mass spectrometer. A silica capillary C18 column (75 μm×25 cm, Thermo, USA) was used for peptide separation, and the flow rate was set at 300 nL/min with mobile phase A consisting of 0.1% formic acid in water and mobile phase B consisting of 0.1% formic acid in 80% acetonitrile. Obtained data were searched in the UniProt database using MaxQuant software.

Molecular docking

A sophisticated protein-protein docking analysis was conducted using the structural data of Adipsin (AlphaFoldDB: P00746) and SERBP1 (AlphaFoldDB: Q8NC51) by HEX 8.0 software (https://hex.loria.fr/). The optimal docking complex was identified and scrutinized through Pymol 2.3.0 for visualization and comprehensive analysis.

RNA sequencing analysis

HUVECs infected with either Ad-Adipsin or Ad-Control were subjected to a high-glucose, hypoxic environment for 24 h. After this exposure, total RNA was extracted from HUVECs using TRIzol reagent (Invitrogen, 15596026, USA). Genes with significant differential expression were identified using a cutoff fold change≥1.5 and adjusted $p<0.05$. Gene set enrichment analysis (GSEA) was performed using the MSigDB. All bioinformatics analyses were conducted on the integrated cloud platform of Majorbio (https://cloud.majorbio.com/) [24].

Statistical analysis

All data are presented as scatter dot plots or line charts with mean±SEM, and $p<0.05$ was considered significant. Detailed information regarding the number of independent biological samples or mice used in each experiment, as well as the frequency with independently repetitions, is provided in the corresponding figure legends. The Shapiro-Wilk test was employed to assess data normality, while the Brown-Forsythe test was used to evaluate the homogeneity of variance. Upon verifying the assumptions of homogeneity of variances and normality, the statistical comparisons were conducted as follows: For comparisons between two groups, a two-tailed Student's unpaired t-test was employed. For comparisons involving multiple groups, one-way ANOVA followed by Tukey's multiple comparison test was utilized. In experiments incorporating a second variable, two-way ANOVA with Tukey's multiple comparison test was performed. Specifically, for Laser Doppler imaging experiments,

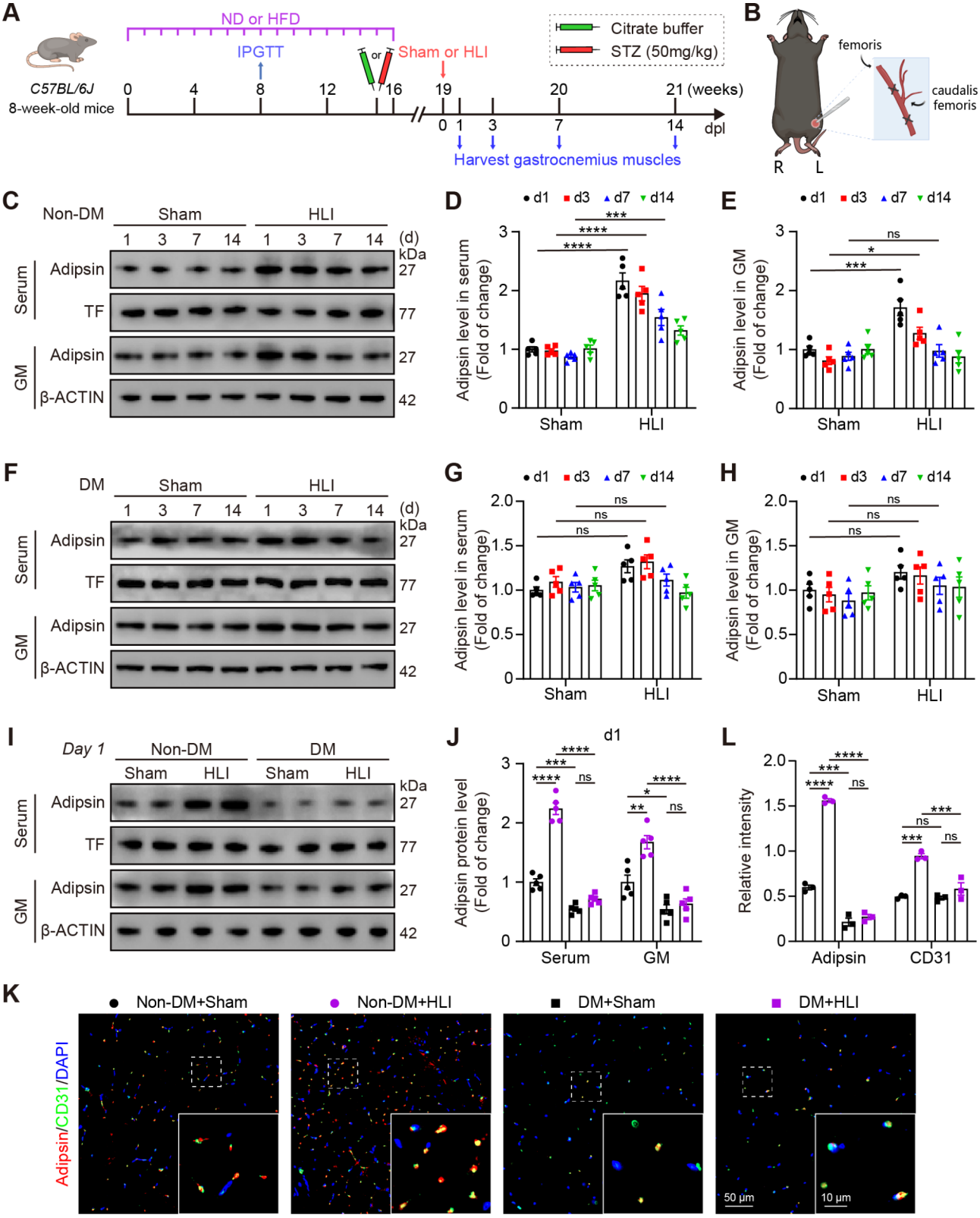

Fig. 1 (See legend on next page.)

(See figure on previous page.)

Fig. 1 Adipsin is upregulated in HLI model although it is suppressed under diabetic conditions. **A** Experimental scheme of establishment of T2DM in mice and femoral artery ligation to mice. **B** Schematic graphic of ischemia model used in this model. **C** Serum, and gastrocnemius muscles (GM) were harvested from non-diabetic mice at the specified time points following either HLI or sham operation. Expression level of Adipsin were quantified using Western blotting. **D**, **E** Quantification of Adipsin/TF (**D**), Adipsin/β-ACTIN (**E**) ($n = 5$ mice). **F** Serum, and GM were harvested from diabetic mice at the specified time points following either HLI or sham operation. Expression level of Adipsin were determined using Western blotting. **G**, **H** Quantification of Adipsin/TF (**G**), Adipsin/β-ACTIN (**H**) ($n = 5$ mice). **I** Representative Western blot images of serum and GM Adipsin levels at 1-day post femoral artery ligation (dpl) or sham operation control. **J** Quantification of Adipsin/TF, Adipsin/β-ACTIN ($n = 5$ mice). **K** Representative immunofluorescence images of Adipsin and CD31 in GM at 3 dpl. **L** Quantitative analysis of Adipsin and CD31 in GM ($n = 3$ mice). Values are presented as mean ± SEM in **D**, **E**, **G**, **H**, **J** and **L**. Statistical significance is determined using two-way ANOVA followed by a Tukey *post hoc* test in **D**, **E**, **G**, **H**, **J** and **L**. $^{*}p < 0.05$, $^{**}p < 0.01$, $^{***}p < 0.001$, $^{****}p < 0.0001$

two-way repeated measures ANOVA with Tukey's multiple comparison test was applied. All statistical analyses were conducted using GraphPad Prism 9 (GraphPad Software, CA).

Results

Adipsin is upregulated in HLI model yet suppressed under diabetic conditions

Diabetes is implicated in the development of PAD. Our previous studies have shown a cardioprotective property for Adipsin in improving cardiac function in DCM [10, 19]. However, the effect of Adipsin on post-ischemic blood flow recovery is not well understood. We evaluated whether Adipsin expression remained stable or was regulated under pathological conditions. In this study, we induced a diabetic mouse model using HFD/STZ induction, and established hindlimb ischemia (HLI) by ligating the left femoral artery (Fig. 1A, B). Adipsin protein levels were monitored in serum and gastrocnemius muscles of C57BL/6 mice at 1, 3, 7, and 14 days post-ligation (dpl). When subjected to HLI, Adipsin levels in the serum and gastrocnemius muscles were significantly upregulated in non-diabetic mice (Non-DM), compared to sham controls (Fig. 1C–E). However, this induction of Adipsin by ischemia was abolished in diabetic mice (DM) (Fig. 1F–H), suggesting a potential role for Adipsin in ischemic recovery that is impaired in diabetic mice. Consistent with our previous observation, levels of Adipsin in serum and gastrocnemius muscles were lower in diabetic mice compared to non-diabetic mice (Fig. 1I, J). Intriguingly, immunofluorescence analysis demonstrated that Adipsin predominantly co-localized with the endothelial cell marker CD31. Furthermore, Adipsin fluorescence intensity in gastrocnemius muscles showed a pronounced increase in Adipsin signal post-femoral artery ligation as compared to the sham-operated group. In contrast, no such elevation in Adipsin levels was observed in diabetic mice (Fig. 1K, L). Consequently, we hypothesized that Adipsin might play a pivotal role in regulating blood perfusion restoration and tissue regeneration following hindlimb ischemia.

To determine the possible role of Adipsin in blood perfusion recovery, we generated heterozygous mice with conditional Adipsin overexpression. Adipose tissue-specific Adipsin transgenic mice (Adipsin-Tg) were created by crossing conditional Rosa26 Adipsin knock-in homozygous ($Adipsin^{LSL/LSL}$Tg) mice with Adipoq-Cre mice [19]. Western blot and quantitative real-time PCR verified the intended overexpression in transgenic mice, evidenced by increased levels of *Adipsin* mRNA in white adipose tissue (WAT) and Adipsin protein in serum and gastrocnemius muscles (Supplementary Material 2: Fig. S1A–D), validating successful generation of Adipsin-Tg mice. Further analysis of gastrocnemius muscles demonstrated little differences in capillary density and arteriolar number (Supplementary Material 2: Fig. S1E–H) between NTg and Adipsin-Tg mice in the absence of hindlimb ischemia challenge.

Adipsin facilitates the restoration of blood flow and promotes angiogenesis in diabetic HLI

To determine whether Adipsin plays a role in protecting against diabetic ischemia, NTg and Adipsin-Tg mice were randomly grouped in a 1:1 ratio treated with ND/citrate buffer (Non-DM + NTg, Non-DM + Adipsin-Tg) or HFD/STZ (DM + NTg, DM + Adipsin-Tg) (Fig. 2A). No significant differences were observed in blood glucose levels and glucose tolerance between NTg and Adipsin-Tg mice, with or without diabetes (Supplementary Material 2: Fig. S2A–C). Mice were then subjected to hindlimb ischemia by ligation of the femoral artery. Blood flow recovery was quantified using PSI at 0, 3, 7, and 14 dpl (Fig. 2B, C and Supplementary Material 2: Fig. S2D, E). Laser Doppler perfusion images showed that the surgical procedure reduced blood flow in the ischemic hindlimbs, while diabetes remarkably impaired blood flow recovery. However, Adipsin overexpression remarkably accelerated blood flow recovery at 7 and 14 dpl compared to diabetic NTg mice. Notably, diabetic mice displayed significantly impaired limb function compared to non-diabetic mice, with significantly increased number of necrotic toes (Supplementary Material 2: Fig. S2F, G). Adipsin-Tg mice exhibited an increased frequency of necrotic toes, concomitant with improved functional outcomes in their hindlimbs of diabetic animals. These results indicate that Adipsin improves blood flow recovery and function in diabetic mice with HLI.

To elucidate the underlying mechanisms through which Adipsin facilitates the restoration of blood perfusion in lower extremities with ischemia, H&E staining

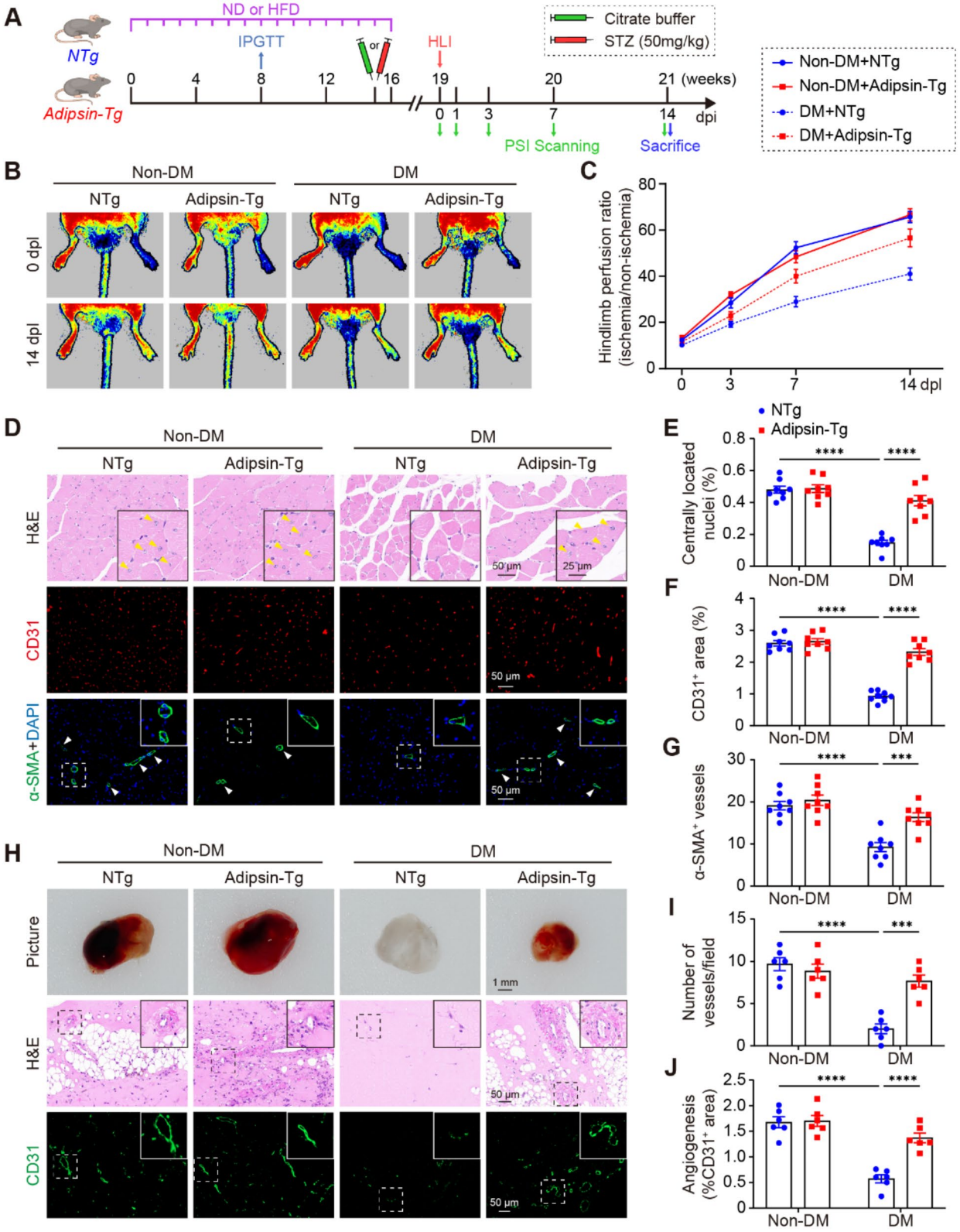

Fig. 2 (See legend on next page.)

(See figure on previous page.)

Fig. 2 Adipsin facilitates restoration of blood flow and promotes angiogenesis in diabetic HLI. **A** Experimental schematic illustrating the establishment of T2DM mice and the procedure for femoral artery ligation. **B** Representative images illustrating blood flow in the hindlimb paws, monitored by PeriCam PSI at 0 and 14 days post-ligation (dpl). **C** Quantification of blood flow recovery at 0, 3, 7, and 14 dpl, as assessed by the ischemic to non-ischemic limb perfusion ratio. Values are presented as mean ± SEM ($n = 8$ mice). Statistical significance is determined using two-way repeated measures ANOVA followed by a Tukey *post hoc* test. **D** Representative images of H&E staining of gastrocnemius muscle sections at 14 dpl. **E** Quantification of the number of newborn skeletal muscle cells ($n = 8$ mice). **F** Quantification of CD31-positive area ($n = 8$ mice). **G** Quantification of α-SMA-positive vessels count ($n = 8$ mice). **H** Representative images of Matrigel plugs encompassing photographic, H&E staining, and immunostaining analysis of blood vessels. (Top row) Depicts representative photographs of Matrigel plugs collected at 14 days post-implantation. (Middle row) Illustrates histological examination of the Matrigel plugs using H&E staining. (Bottom row) Showcases representative images of Matrigel plugs subjected to immunostaining for CD31. **I** Quantification of the number of blood vessels in the H&E-stained Matrigel plugs ($n = 8$ mice). **J** Quantification of angiogenesis in Matrigel plugs by measuring CD31-positive area ($n = 8$ mice). Values are presented as mean ± SEM in **C**, **E**, **F**, **G**, **I** and **J**. Statistical significance is determined using two-way ANOVA followed by Tukey *post hoc* test in **E**, **G**, **I**, **K** and **L**. *$p < 0.05$, **$p < 0.01$, ***$p < 0.001$, ****$p < 0.0001$

and immunofluorescence labeling of CD31 and α-smooth muscle actin (α-SMA) were conducted in the ischemic skeletal muscles (Fig. 2D). Histological analysis of muscle sections indicated that impaired regeneration of the gastrocnemius muscle in hindlimb ischemia diabetic mice was largely restored by Adipsin overexpression, as manifested by a significant increase in myocytes exhibiting centrally positioned nuclei (Fig. 2E). In addition, immunofluorescence assay of ischemic tissue revealed that diabetic Adipsin-Tg mice exhibited increased capillary density and arteriolar abundance in the gastrocnemius muscles at 14 dpl compared to NTg mice. (Fig. 2F, G). These data suggest that Adipsin promotes angiogenesis in diabetic mice following ischemic injury.

To further confirm this phenotype, the Matrigel plug assay, a widely used ex vivo model for assessing angiogenesis was utilized to discern the potential impact of Adipsin overexpression on angiogenesis. Consistent with earlier findings, Adipsin was found to enhance hemoglobin content (Fig. 2H and Supplementary Material 2: Fig. S2H) and promote vessel formation (Fig. 2H–J) as evidenced by bright-field imaging, H&E staining and immunostaining of CD31. These findings were in line with the increased angiogenesis observed in diabetic Adipsin-Tg mice following HLI, providing strong evidence for the promotion of angiogenesis by Adipsin overexpression. These results collectively favor a crucial role for Adipsin in promoting post-ischemic angiogenesis and facilitating blood perfusion recovery, thereby leading to improved tissue repair following HLI.

Adipsin enhances the migration, proliferation, and angiogenic activity of HUVECs under diabetic conditions

To further assess the cellular effect of Adipsin under diabetic, ischemia-simulating conditions, HUVECs were transfected with an Adipsin-overexpressing adenovirus (Ad-Adipsin) or an empty adenovirus (Ad-Control). Transfection efficiency was assessed (Supplementary Material 2: Fig. S3A–D). Subsequently, HUVECs were subjected to hypoxic conditions (HG-HY) in the presence of 25 mM glucose or normoxic conditions (NG-NO) with 5 mM glucose (Fig. 3A). Angiogenesis, the process by which new blood vessels form, depends on the budding, proliferation, and migration of endothelial cells. To this end, HUVEC viability was assessed using the Cell Counting Kit-8 assay across various experimental groups. HG-HY treatment resulted in reduced HUVEC viability, whereas Adipsin significantly increased their viability under HG-HY conditions (Fig. 3B). Moreover, Adipsin overexpression rescued the proliferation capacities of HUVECs as confirmed by EdU incorporation assay (Fig. 3C, D). Moreover, the influence of Adipsin on the migration capacity of HUVECs was evaluated in vitro using wound healing and transwell assays. The wound healing assay revealed that HUVECs exposed to HG-HY conditions exhibited a significantly reduced migration area as compared to the NG-NO group, whereas Adipsin markedly enhanced the migration area of HUVECs under HG-HY conditions (Fig. 3E, F). Results from the transwell assay denoted that Adipsin effectively counteracted the impaired cell migration evoked by HG-HY and significantly enhanced migration of HUVECs challenged with HG-HY compared to the control group (Fig. 3G, H). Tube formation assay was executed to evaluate the ability of Adipsin to promote HUVECs angiogenesis. As expected, HG-HY treatment led to a significant reduction in both total tube length and meshed area. Interestingly, Adipsin reversed these effects and significantly promoted tube formation under HG-HY conditions (Fig. 3I–K). Taken together, these data suggest a regulatory role for Adipsin in endothelial cell biological functions essential for angiogenesis, including cell proliferation, migration, and tube formation.

Adipsin markedly downregulates SERPINE1 and its downstream genes in HUVECs

We aimed to uncover the molecular mechanisms underlying the effects of Adipsin on endothelial cells under ischemic conditions. Therefore, HUVECs infected with Ad-Adipsin or Ad-Control were exposed to a high-glucose hypoxic environment for 24 h prior to collection of cells for RNA-sequencing analysis (Fig. 4A). Analysis of differentially expressed genes, using a cut-off fold change ≥ 1.5, as well as adjusted p value < 0.05,

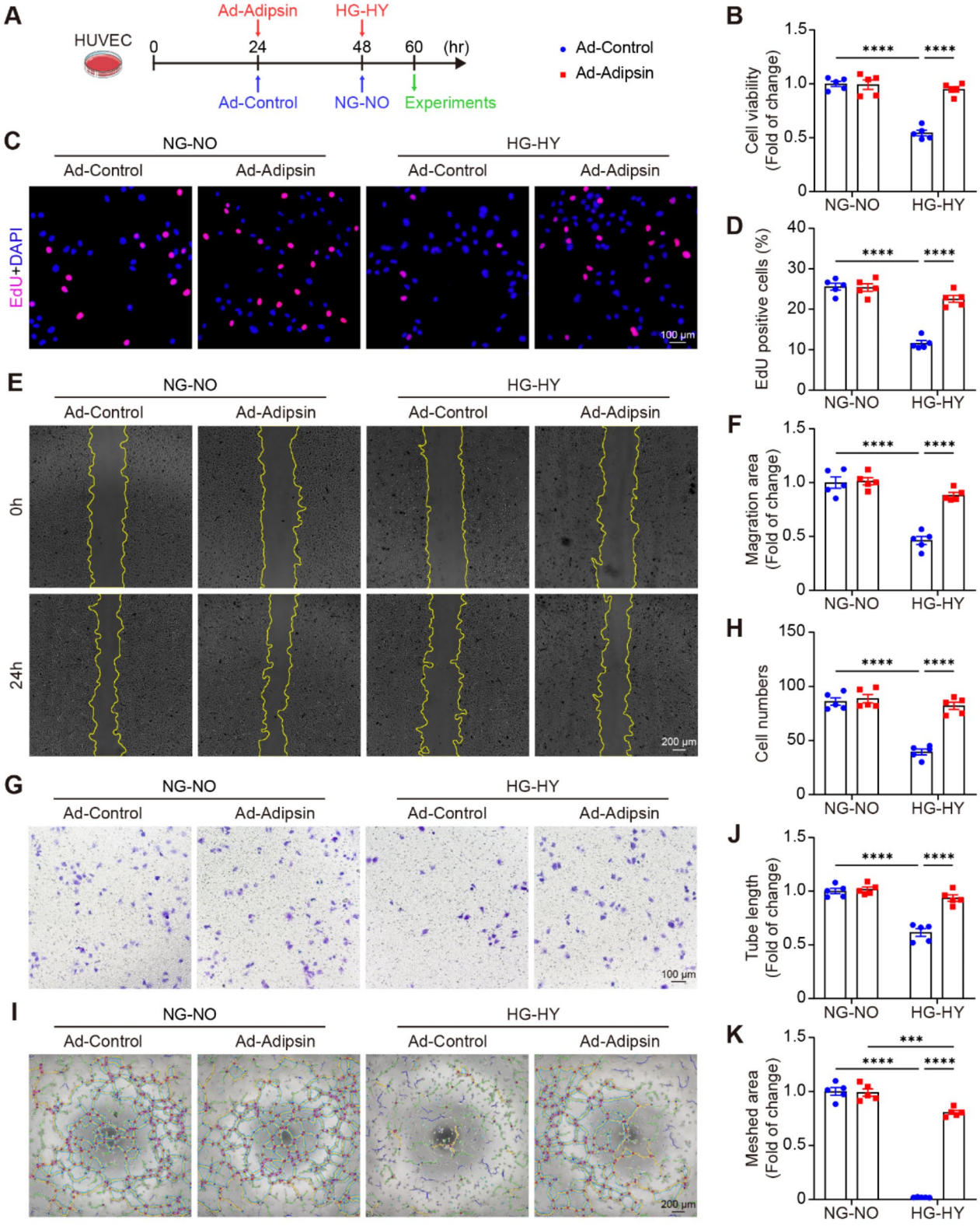

Fig. 3 (See legend on next page.)

(See figure on previous page.)

Fig. 3 Adipsin enhances the migration, proliferation, and angiogenic activity of HUVECs under diabetic conditions. **A** Experimental design for **B** through **K**. HUVECs were infected with either Ad-Adipsin or Ad-Control for 24 h, and were then incubated in a high-glucose medium (25 mM) within a hypoxic chamber or subjected to hypoxia with 5 mM glucose for 12 h. **B** Cell viability of HUVECs infected with Ad-Adipsin or Ad-Control with or without HG-HY treatment determined using CCK-8 assay ($n=3$). **C** Representative images of HUVECs proliferation examined by EdU incorporation assay. **D** Plot showing the quantification of EdU-positive cells ($n=3$). **E** Migration of HUVECs was measured using wound healing assay. Yellow line indicated the boundary of scratch. **F** Plot exhibiting analysis of migration area ($n=3$). **G** Representative images of migrating HUVECs. **H** Plot showing the number of migrated cells ($n=3$). **I** Representative images of tube formation in a Matrigel assay. Vascular network was segmented using the ImageJ software for better visualization. **J**, **K** Plot exhibiting analysis of total tube length (**J**) and meshed area (**K**) ($n=3$). Values are presented as mean ± SEM in **B**, **D**, **F**, **H**, **J** and **K**. Statistical significance is determined using two-way ANOVA followed by a Tukey *post hoc* test in **B**, **D**, **F**, **H**, **J** and **K**. *$p<0.05$, **$p<0.01$, ***$p<0.001$, ****$p<0.0001$

which revealed 141 upregulated genes and 70 downregulated genes in response to Adipsin overexpression, as depicted in a volcano plot (Fig. 4B). The global gene expression profiles from RNA-sequencing (RNA-seq) indicated extensive activation of angiogenesis-related signaling cascades in Ad-Adipsin treated HUVECs compared to control HUVECs under HG-HY conditions (Fig. 4C). The transcriptomics study revealed that VEGF signaling and PI3K-Akt signaling may serve as targets of Adipsin for promoting angiogenesis. To this end, we examined whether Adipsin affects VEGF-induced downstream PI3K-AKT activation. As expected, AKT, ERK, and eNOS were activated upon VEGF activation. Our results revealed that Adipsin enhanced activation of AKT, ERK, and eNOS in HUVECs in response to VEGF stimulation (Fig. 4D, E). Previous studies have shown that VEGF-induced activation of PI3K-Akt signaling cascade requires VEGFR2 dimerization and autophosphorylation, thereby modulating endothelial angiogenesis [25–27]. Indeed, Western blot analysis revealed that Adipsin overexpression facilitated VEGFR2 phosphorylation upon VEGF stimulation in HUVECs under HG-HY conditions (Fig. 4F, G).

Interestingly, analysis of gene expression indicated a significant decrease in *SERPINE1* expression in HUVECs infected with Ad-Adipsin under high-glucose hypoxic conditions (Fig. 4B). Furthermore, it was shown that SERPINE1 inhibits activation of VEGFR2 induced by VEGF, through disruption of a vitronectin-dependent proangiogenic binding interaction between αVβ3 integrin and VEGFR-2 [28]. Consequently, it impedes both cell adhesion and migration, thereby leading to inhibition of angiogenesis [29]. Therefore, we hypothesized that Adipsin might promote angiogenesis by modulating SERPINE1 to regulate VEGF-A/VEGFR2 signaling. As expected, SERPINE1 expression was decreased in HUVECs infected with Ad-Adipsin under HG-HY conditions (Fig. 4F, G). These results were consistent with in vivo data, with significantly lower levels of SERPINE1 protein in diabetic Adipsin-Tg group compared to diabetic NTg group at 7 dpl. Additionally, Adipsin increased the phosphorylation of the aforementioned proteins in diabetic ischemic muscles (Fig. 4H, I).

SERPINE1 mediates Adipsin-induced angiogenesis in diabetic mice subjected to hindlimb ischemia

To further explore the role of SERPINE1 in Adipsin-induced angiogenesis following ischemia in vivo, adeno-associated virus-1 (AAV1) carrying sh*RNA* targeting *Serpine1* was used to knockdown its expression in mice (Supplementary Material 2: Fig. S4B, C). Two weeks later, femoral artery ligation was performed, and subsequent examination involved laser Doppler perfusion imaging and molecular biological evaluation at designated time points (Fig. 5A). Our findings demonstrated that blood flow recovery in the ischemic hindlimb was significantly enhanced in diabetic NTg mice with Serpine1 knockdown as compared to control mice that received AAV1-sh*N* injection. Notably, overexpression of Adipsin failed to further improve blood flow recovery in diabetic mice with SERPINE1 knockdown, indicating that Adipsin-induced responses are mediated by the downstream effects of SERPINE1 (Fig. 5B–D). Both H&E staining and immunofluorescence analysis revealed that knockdown of Serpine1 enhanced gastrocnemius muscle regeneration, capillary density, and arteriolar count in hindlimb ischemic diabetic mice. In contrast, overexpression of Adipsin did not offer additional improvement to these responses (Fig. 5E–H). Our findings collectively suggest that Adipsin promotes angiogenesis in diabetic mice with hindlimb ischemia, partially through regulation of SERPINE1 expression.

SERPINE1 mediates Adipsin-induced cellular effects in HUVECs

In vitro cell experiments were conducted using HUVECs infected with Ad-Adipsin or Ad-Control for 24 h. Then, a small interfering RNA (siRNA)-based approach was employed to knock down *SERPINE1* in HUVECs maintained in high-glucose hypoxic conditions (Supplementary Material 2: Fig. S4A). In alignment with in vivo findings, knockdown of SERPINE1 notably enhanced growth, migration, and tube formation in HUVECs. Moreover, Adipsin overexpression did not offer further improvement in endothelial cell function following SERPINE1 knockdown (Supplementary Material 2: Fig. S4D–K). These findings suggest that Adipsin enhances endothelial cell functions in diabetic conditions, and

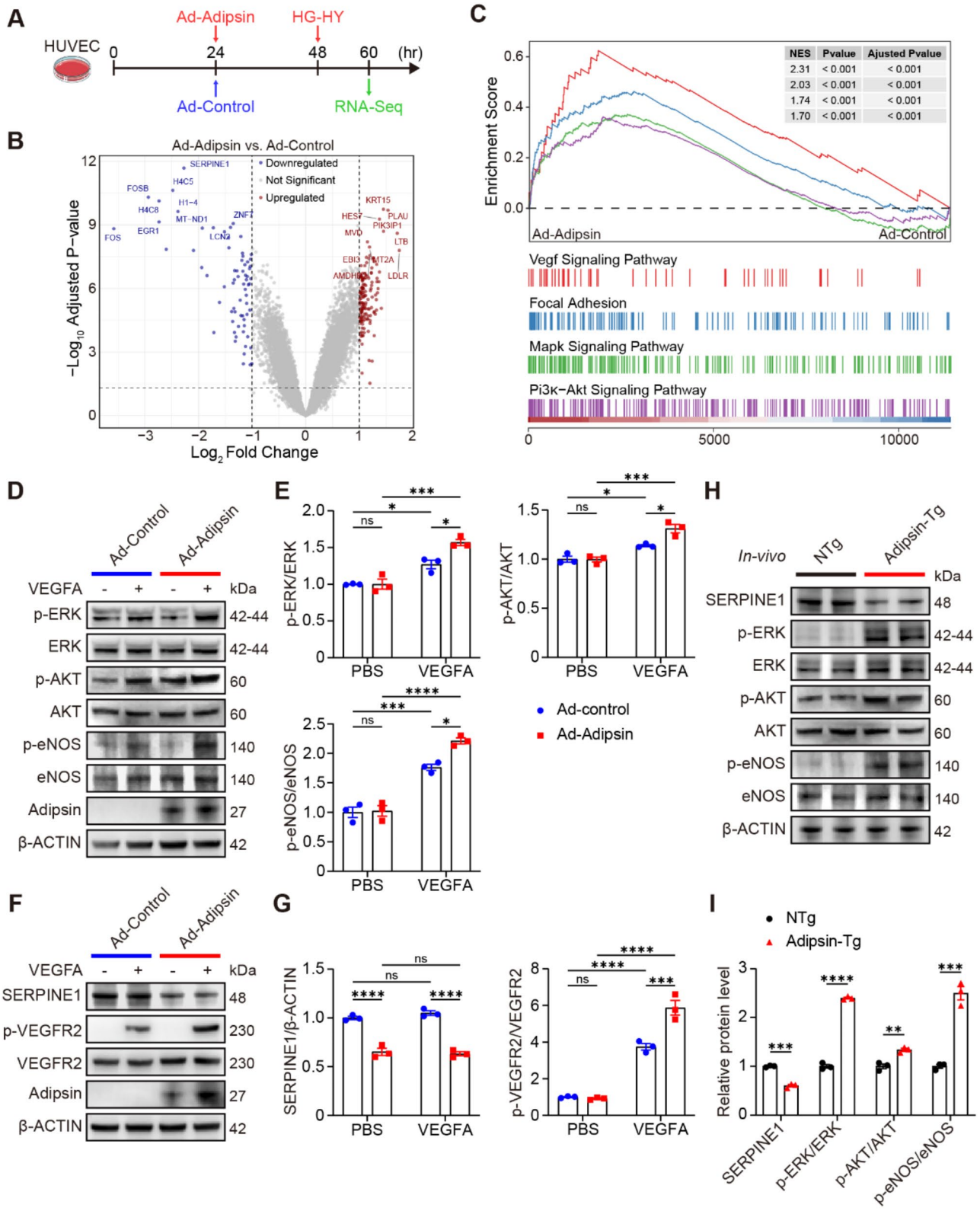

Fig. 4 (See legend on next page.)

(See figure on previous page.)

Fig. 4 Adipsin markedly downregulates SERPINE1 and its downstream genes in HUVECs. **A** Scheme depicting workflow of harvesting HUVECs for RNA sequencing analysis. **B** Volcano plot of RNA-seq data comparing Ad-Adipsin versus Ad-Control groups reveals differentially expressed genes (DEGs). Genes with fold-change ≥ 1.5 and adjusted $p < 0.05$ were considered significantly DEGs. Red, green, and gray dots represent significantly upregulated, downregulated, and not significantly altered genes, respectively. **C** Enrichment of pathways related to angiogenesis in the control or Adipsin-overexpressed HUVECs of HG-HY treatment, as analyzed by GSEA of RNA-seq data. **D** Control or Adipsin-overexpressed HUVECs were treated with or without VEGF-A stimulation (50 ng/mL) for 5 min. Cell lysates were subsequently subjected to immunoblotting with antibodies specific for p-ERK, ERK, p-AKT, AKT, p-eNOS, and eNOS. The experiments were conducted independently in triplicate. **E** Quantification of p-ERK/ERK, p-AKT/AKT, and p-eNOS/eNOS ($n = 3$). **F** Control or Adipsin-overexpressed HUVECs were treated with or without VEGF-A stimulation (50 ng/mL) for 5 min. Cell lysates were subsequently subjected to immunoblotting with antibodies specific for SERPINE1, p-VEGFR2, and total VEGFR2. **G** Quantification of SERPINE1/β-ACTIN and p-VEGFR2/VEGFR2 ($n = 3$). **H** Gastrocnemius muscles were harvested from diabetic NTg and Adipsin-Tg mice at 7 dpl. Expression level of SERPINE1, p-ERK, ERK, p-AKT, AKT, p-eNOS, and eNOS were determined using Western blotting. **I** Quantification of SERPINE1/β-ACTIN, p-ERK/ERK, p-AKT/AKT, and p-eNOS/eNOS ($n = 3$). Values are presented as mean ± SEM in **E**, **G**, and **I**. Statistical significance is determined using two-tailed Student's unpaired t-test in **I** or one-way ANOVA followed by a Tukey *post hoc* test in **E**, and **G**. *$p < 0.05$, **$p < 0.01$, ***$p < 0.001$, ****$p < 0.0001$

SERPINE1 serves as a downstream regulator for Adipsin in the process of angiogenesis.

Adipsin interacts with SERBP1 within the cytoplasm

To comprehend the mechanism through which Adipsin enhances downregulation of SERPINE1 and to identify additional proteins that possibly interact with Adipsin, a co-immunoprecipitation/mass spectrometry (Co-IP/MS) experiment was conducted. HUVECs were initially treated with Ad-Adipsin under conditions of high-glucose hypoxia. A Co-IP assay was then performed using Adipsin as a target protein, followed by LC-MS/MS analysis to find co-binding proteins for Adipsin (Fig. 6A). Among the identified proteins, SERBP1 (SERPINE1 mRNA binding protein 1) was of particular interest given its known role in the regulation of mRNA stability of *SERPINE1* (Supplementary Material 1: Table S5) [30]. Thus, SERBP1 was selected for further investigation. To elucidate the potential interaction between Adipsin and SERBP1 in Ad-Adipsin infected HUVECs, Co-IP assays were conducted using antibodies against Adipsin and SERBP1. This resulted in a notable interaction being detected between Adipsin and SERBP1 (Fig. 6B, C). Moreover, confocal microscopy analysis revealed that Adipsin and SERBP1 co-localized in the cytoplasm of HUVECs (Fig. 6D, E). Computer-aided molecular docking was employed to predict possible interaction sites between Adipsin and SERBP1 (Fig. 6F).

We then evaluated whether SERBP1 expression remained stable or was regulated under pathological conditions. In this study, we examined microarray and RNA sequencing datasets from public databases (GSE3313, GSE152139, GSE49524). The analysis revealed that SERBP1 expression in muscles remained stable in mice subjected to HLI, as compared to pre-HLI group (Supplementary Material 2: Fig. S5A, B). Similarly, there was no alteration in SERBP1 expression in adductor muscle of Lepr db/db mice or in HUVECs derived from women with gestational diabetes (Supplementary Material 2: Fig. S5C, D). As a validation, both qPCR and western blot analysis showed that SERBP1 expression did not exhibit significant variation in HUVECs under high glucose-hypoxic conditions (Supplementary Material 2: Fig. S5E–G). In alignment with in vitro findings, there was no detectable alteration of SERBP1 expression in muscles of mice suffering from hindlimb ischemia or hyperglycemia (Supplementary Material 2: Fig. S5H, I).

A subsequent study was conducted to determine whether the interaction between Adipsin and SERBP1 influences the mRNA stability of *SERPINE1*. Overexpression of Adipsin led to a reduction in the mRNA level of *SERPINE1*. Similarly, the inhibition of SERBP1 also correlated with a decrease in *SERPINE1* mRNA (Fig. 6G, H). Moreover, with the usage of actinomycin D to inhibit RNA synthesis, the mRNA levels of *SERPINE1* displayed a decreased pattern upon the overexpression of Adipsin and the half-life of *SERPINE1* mRNA diminished following silencing of SERBP1 (Fig. 6I, J). Importantly, western blot analysis showed that Adipsin treatment did not affect the SERBP1 protein levels in diabetic mice at 7 dpl, indicating that the observed effects on mRNA stability were not due to alterations in SERBP1 expression (Supplementary Material 2: Fig. S5J, K). These findings elucidate a previously unrecognized post-transcriptional regulatory mechanism. A direct interaction was discerned between Adipsin and SERBP1, leading to diminished binding between SERBP1 and *SERPINE1* mRNA, thereby destabilizing *SERPINE1* mRNA expression.

Adipsin mediates angiogenesis through its interaction with SERBP1

We subsequently evaluated if the interaction between Adipsin and SERBP1 is crucial for Adipsin-potentiated angiogenesis. AAV1-Serbp1-sh*RNA* or control AAV1-negative control (NC)-sh*RNA* was administered into the gastrocnemius muscles of the Adipsin-transgenic and non-transgenic diabetic mice bi-laterally, two weeks prior to HLI, to downregulate SERBP1 expression (Fig. 7A and Supplementary Material 2: Fig. S6B, C). Perfusion measurements of the hindlimb revealed an enhancement in the recovery of blood flow in the ischemic limb following suppression of SERBP1 expression. However, overexpression of Adipsin did not provide additional benefits in the recovery of blood flow in diabetic mice where SERBP1

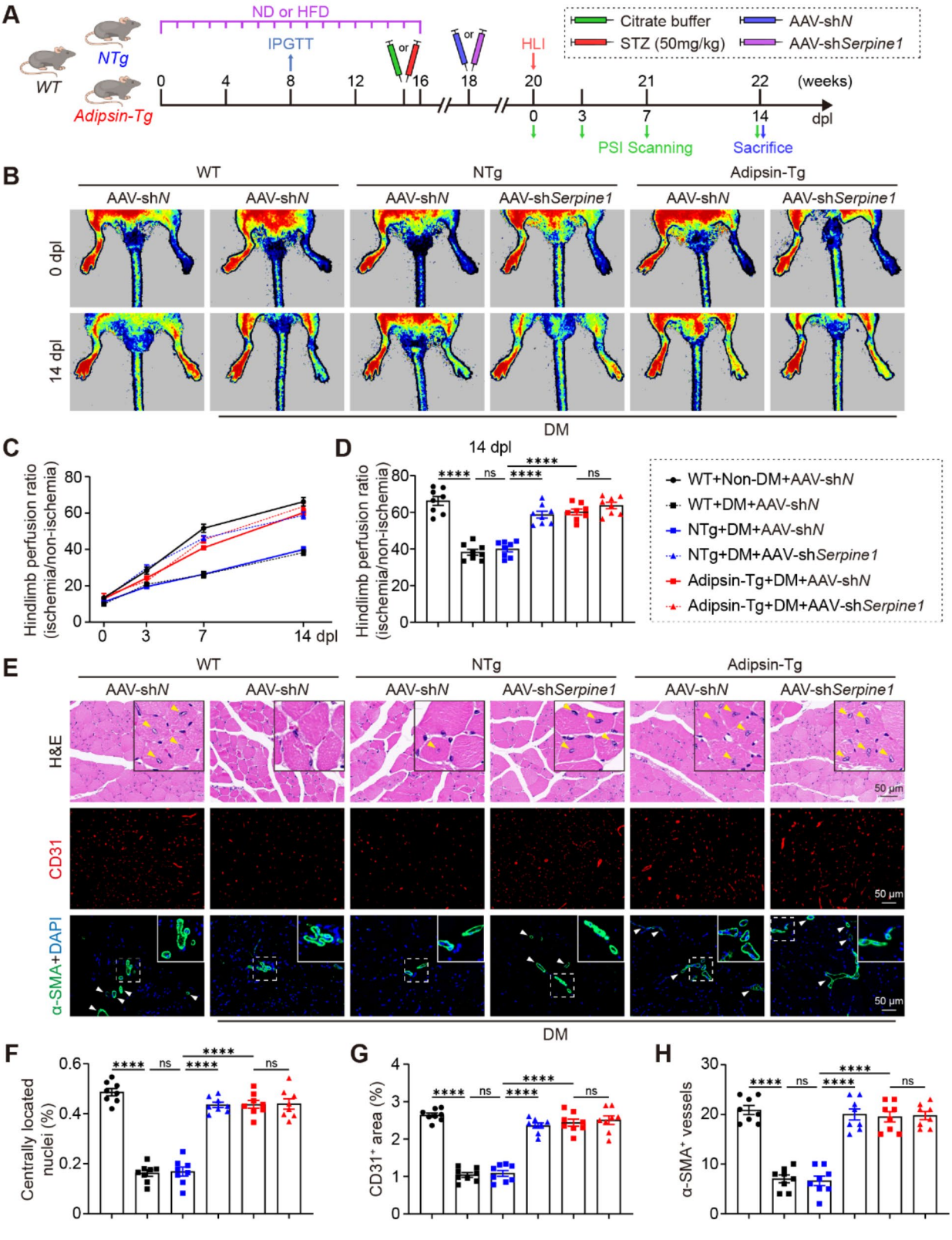

Fig. 5 (See legend on next page.)

(See figure on previous page.)

Fig. 5 SERPINE1 mediates Adipsin-induced angiogenesis in diabetic mice subjected to hindlimb ischemia. **A** Experimental schematic depicting the establishment of T2DM mouse model, administration of AAV1, and procedure for femoral artery ligation. **B** Representative images illustrating blood flow in hindlimb paws, as monitored by PeriCam PSI at 0 and 14 days post-ligation (dpl). **C** Quantification of blood flow recovery at 0, 3, 7, and 14 dpl, assessed by the ischemic to non-ischemic limb perfusion ratio. **D** Blood flow at 14 dpl. Values are presented as mean ± SEM ($n = 8$ mice). Statistical significance is determined using two-way repeated measures ANOVA followed by a Tukey *post hoc* test. **E** Representative images of H&E staining and immunostaining of gastrocnemius muscle sections at 14 dpl. **F** Quantification of the number of newborn skeletal muscle cells ($n = 8$ mice). **G** Quantification of CD31-positive area ($n = 8$ mice). **H** Quantification of α-SMA-positive vessels count ($n = 8$ mice). Values are presented as mean ± SEM in **F**, **G** and **H**. Statistical significance is determined using two-way ANOVA followed by a Tukey *post hoc* test in **F**, **G** and **H**. *$p < 0.05$, **$p < 0.01$, ***$p < 0.001$, ****$p < 0.0001$

was knocked down (Fig. 7B, C and Supplementary Material 2: Fig. S6D, E). The potential effect of SERBP1 on angiogenesis was further corroborated through the Matrigel plug assay. Consistently, knockdown of SERBP1 increased hemoglobin content and promoted vessel formation as depicted using bright-field imaging, H&E staining, and CD31 immunostaining. Overexpression of Adipsin, however, did not offer any further effect on the observed phenomena (Fig. 7D–F and Supplementary Material 2: Fig. S6F).

To validate our hypothesis, additional in vitro assays were conducted to elucidate the role of SERBP1 in HUVECs. The findings from the EdU proliferation, Transwell invasion, wound healing, and tube formation assays affirmed that the knockdown of SERBP1 (Supplementary Material 2: Fig. S6A) significantly stimulated growth and enhanced migration of HUVECs. It was anticipated that Adipsin overexpression did not result in further growth or enhanced migration of HUVECs under high glucose-hypoxic conditions following SERBP1 knockdown (Fig. 7G–J and Supplementary Material 2: Fig. S6G–K). These data indicate that Adipsin prompts angiogenesis in diabetic ischemic hindlimb and suggest the role for SERBP1 as a downstream regulator for Adipsin.

Discussion

Peripheral arterial disease (PAD) is characterized by gradual constriction and occlusion of peripheral arteries, predominantly affecting lower extremities. As a result, the insufficient blood perfusion to the legs precipitates pain, risks of amputation, multi-organ dysfunction, and even mortality [2, 3, 5, 7]. Moreover, among patients afflicted with PAD, individuals with diabetes manifest more pronounced arterial deterioration and endure markedly less favorable prognoses relative to non-diabetic peers [4, 6]. Therapeutic angiogenesis has emerged as a promising strategy for treating lower-limb ischemia [31–33]. Despite the application of VEGF-based monotherapies, clinical outcomes for patients with PAD have remained suboptimal, suggesting the involvement of supplementary regulatory mechanisms in effective angiogenesis [34, 35]. Here in this study, we examined the role of Adipsin in hindlimb ischemia in T2DM mice and the underlying mechanisms involved.

Adipsin, initially described as the first adipokine, is a major protein secreted by adipose cells [14]. Previous research has confirmed that Adipsin is indispensable for the intrinsic alternative complement pathway initiation, as well as the amplification of C3 convertases. These processes participate in the early stages of infection, usually before innate antibodies reaching effective serum levels in circulation [13]. Adipsin has been shown to play important roles in ischemia reperfusion and diabetic cardiomyopathy [17, 19, 36]. Additionally, Adipsin levels were overtly increased in both humans and mice with acute myocardial infarction (MI) [37]. In parallel, our results showed that Adipsin levels were significantly increased in response to ischemic conditions in non-diabetic mice, while failed to exhibit a comparable response in diabetic mice. Moreover, our further study indicated that Adipsin facilitates angiogenesis and restoration of blood flow, thereby promoting tissue repair in diabetic mice following HLI surgery. In vitro studies also denoted that Adipsin promotes proliferation, migration, and tube formation of HUVECs under HG-HY conditions. It is noteworthy that even within an ex vivo environment devoid of complement system components, which are ordinarily indispensable for the conventional functionalities of Adipsin, the exogenously Adipsin overexpression retains the capacity to exert a pronounced effect on HUVECs. These results suggest that Adipsin may have direct effects on promoting angiogenesis in diabetic condition, which is independent of the complement system. Adipsin may serve as a novel therapeutic target for the treatment of PAD. Consistent with previous findings [10, 15, 19, 38], Adipsin levels were overtly decreased in diabetic mice. Importantly, these metabolic improvements may be beneficial for the proangiogenic effect of Adipsin. Our previous study demonstrated that Adipsin overexpression did not significantly affect blood glucose levels in HFD/STZ-induced diabetic group [10]. The observed increase in angiogenesis in response to Adipsin is likely a direct effect in endothelial cells as opposed to a secondary consequence of metabolic improvement.

To unveil the possible molecular mechanisms underneath Adipsin-evoked effect on endothelial cells under high-glucose hypoxic conditions, cells following indicated treatments were subjected to RNA-sequencing analysis. Transcriptomics analysis revealed that VEGF signaling, and PI3K-Akt signaling may serve as targets of Adipsin for promoting angiogenesis. Activation of AKT kinase appears to orchestrate a multitude of signaling

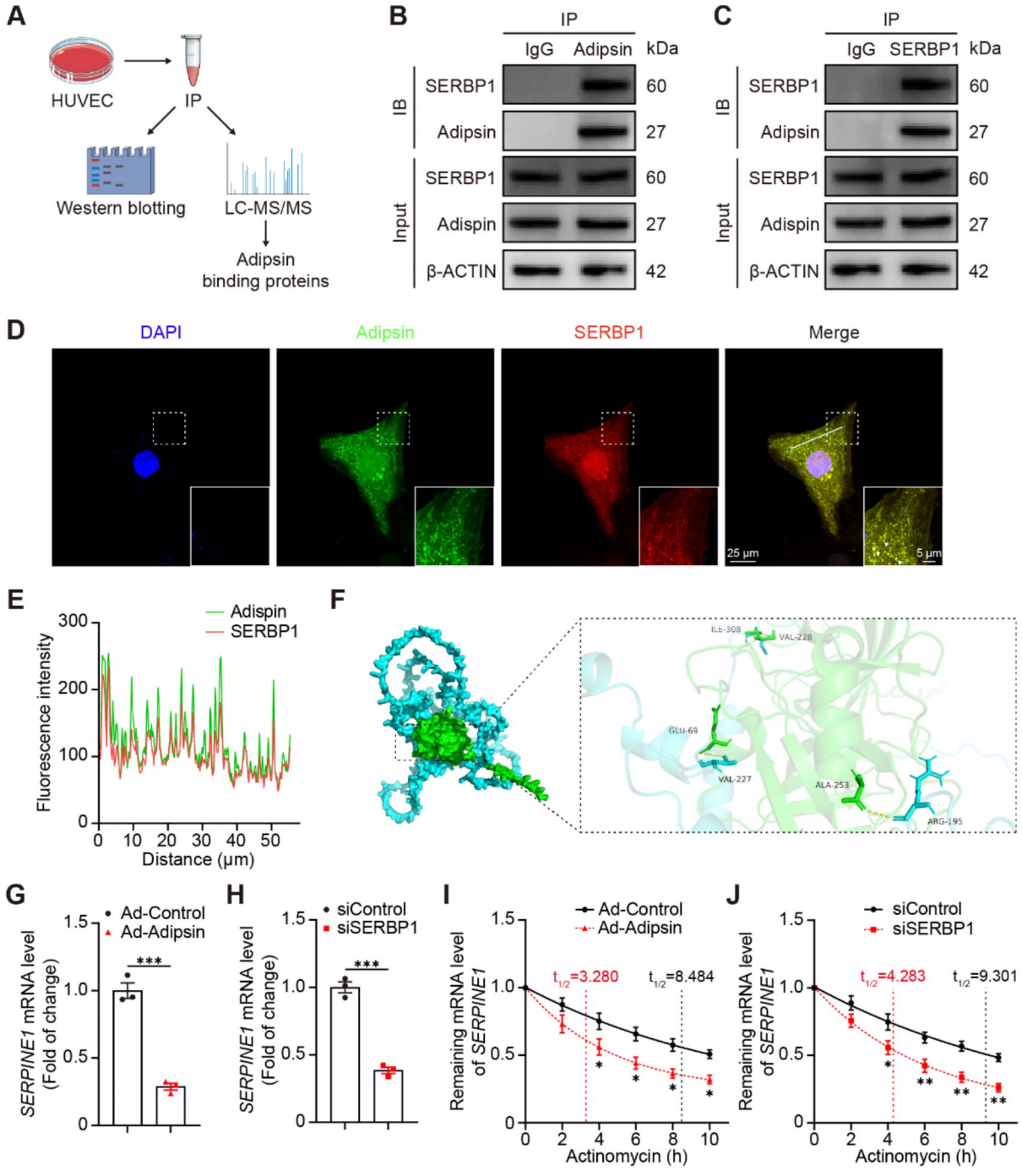

Fig. 6 Adipsin interacts with SERBP1 within the cytoplasm. **A** Schematic representation of the experimental workflow. **B**, **C** Interaction between Adipsin and SERBP1 in HUVECs was validated through Co-IP followed by Western blot analysis ($n=5$). **D** Localization of Adipsin (green) and SERBP1 (red) were stained and visualized using confocal microscopy. **E** Intensity profiles showing colocalization along the direction of the white arrow. **F** Molecular docking analysis of the interaction between Adipsin and SERBP1. **G**, **H** Quantification of *SERPINE1* mRNA levels via RT-qPCR in HUVECs subjected to either Adipsin overexpression or SERBP1 silencing ($n=3$). **I**, **J** Stability of *SERPINE1* mRNA was assessed in HUVECs treated with actinomycin D, following either the overexpression of Adipsin or the silencing of SERBP1 ($n=3$). Values are presented as mean ± SEM in **G**, **H**, **I** and **J**. Statistical significance is determined using two-tailed Student's unpaired t-test in **G** and **H** or two-way repeated measures ANOVA with a Sidak *post hoc* test in **I**, and **J**. *$p<0.05$, **$p<0.01$, ***$p<0.001$, ****$p<0.0001$

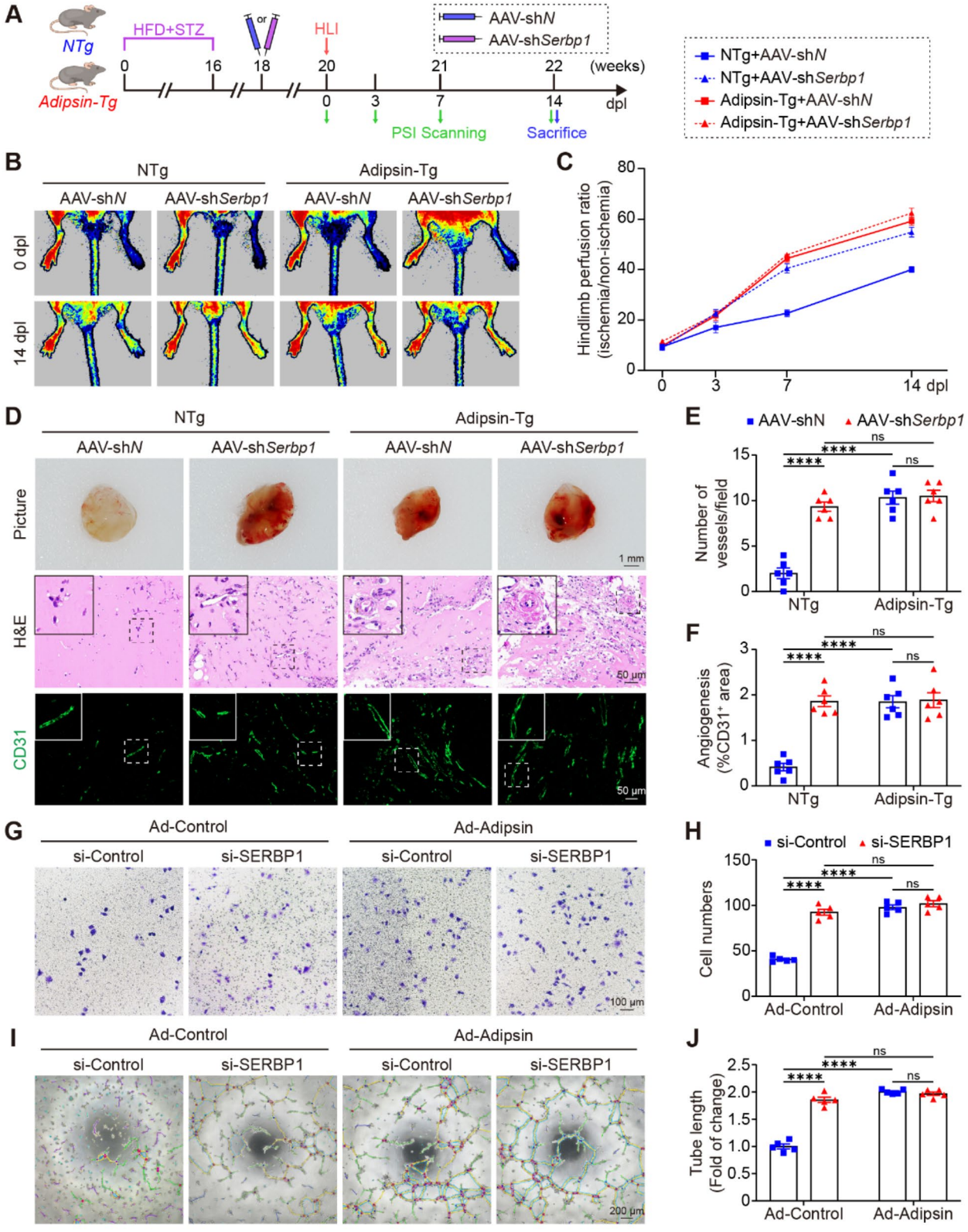

Fig. 7 (See legend on next page.)

(See figure on previous page.)

Fig. 7 Adipsin mediates angiogenesis through its interaction with SERBP1. **A** Schematic representation of the experimental workflow, detailing the establishment of T2DM model, the administration of AAV1, and the procedure for femoral artery ligation. **B** Representative images depicting blood flow in hindlimb paws monitored by PeriCam PSI at 0 and 14 days post-ligation (dpl). **C** Quantification of blood flow recovery at 0, 3, 7, and 14 dpl, as assessed by the perfusion ratio between ischemic and non-ischemic limbs ($n = 8$ mice). Values are presented as mean ± SEM. Statistical significance is determined using two-way repeated measures ANOVA followed by a Tukey *post hoc* test. **D** Representative images of Matrigel plugs, including photographic documentation, H&E staining, and immunostaining analysis of blood vessels. **E** Quantification of the number of blood vessels in the H&E-stained Matrigel plugs ($n = 6$ mice). **F** Quantification of angiogenesis in Matrigel plugs by measuring CD31-positive area ($n = 6$ mice). **G** Representative images of migrating HUVECs. **H** Plot showing the number of migrated cells ($n = 5$). **I** Representative images of tube formation in a Matrigel assay. The vascular network was segmented using the ImageJ software to enhance visualization. **J** Plot showing the analysis of total tube length ($n = 5$). Values are presented as mean ± SEM in **E**, **F**, **H** and **J**. Statistical significance is determined using two-way ANOVA followed by Tukey *post hoc* test in **E**, **F**, **H** and **J**. $^{*}p < 0.05$, $^{**}p < 0.01$, $^{***}p < 0.001$, $^{****}p < 0.0001$

cascades implicated in angiogenesis [39]. The diverse downstream substrates of AKT not only converge to inhibit the induction of apoptosis but may also stimulate proliferation, migration, and tube formation of endothelial cells, ultimately contributing to vascular remodeling and maintenance of vessel integrity throughout the angiogenic process [40–43]. In our hands, Adipsin exerts angiogenic effects in HUVECs by activating AKT, ERK, and eNOS. Previous studies have depicted that VEGF-induced activation of PI3K-Akt signaling requires VEGFR2 dimerization and autophosphorylation, thereby modulating endothelial angiogenesis [25–27]. Our in vitro findings suggested that Adipsin overexpression increased VEGFR2 phosphorylation in response to VEGF stimulation.

Interestingly, we found decreased SERPINE1 expression in HUVECs infected with Ad-Adipsin under high-glucose hypoxic conditions. SERPINE1, also known as plasminogen activator inhibitor-1 (PAI-1), serves as the master regulator of the plasminogen system [44]. It has been implicated for its role in exacerbating diverse pathological conditions through the accumulation of extracellular matrix (ECM), as well as its role in altering cell fate and behavior [45]. Earlier results indicated that the concentration of SERPINE1 increases during the impaired glucose tolerance stage and continues to rise throughout the progression of diabetes and metabolic syndrome [46, 47]. Accumulating evidence has elucidated a vital role for SERPINE1 in promoting angiogenesis and tissue regeneration [28, 48–51]. Moreover, the antiangiogenic effect of SERPINE1 appears to be mediated by modulating VEGF-induced endothelial cell activation through disruption of VEGFR2-αVβ3 crosstalk [29, 52]. These findings further intimated a partial regulatory role for SERPINE1 in Adipsin-induced angiogenesis. In this study, SERPINE1 knockdown exhibited reduced ischemic damage following HLI, which was attributed to augmented blood flow recovery, enhanced angiogenesis, and improved endothelial cell functions, including proliferation, migration, and tube formation. Furthermore, our findings revealed that overexpression of Adipsin did not offer any additional protective effects with suppression of SERPINE1.

We observed that Adipsin directly binds to SERBP1 in HUVECs, offering the specific molecular mechanisms by which Adipsin promotes angiogenesis. SERBP1 is the RBP to regulate mRNA stability of *SERPINE1* [30, 53]. Previous findings have indicated that an association between SERBP1 gene polymorphisms and ischemic stroke risk or clinical manifestations [54]. SERBP1 may modulate proliferation, migration and invasion of lung adenocarcinoma cells via enhancing the mRNA stability of *SERPINE1* [53]. These properties of SERBP1 support its involvement in the regulation of Adipsin to promote angiogenesis and tissue repair. Consistent with these findings, mRNA levels of *SERPINE1* exhibited a pattern of decline upon Adipsin overexpression and the half-life of *SERPINE1* mRNA diminished following SERBP1 silencing. Our results indicated that the reduction of SERBP1 facilitated blood flow recovery, augmented angiogenesis, and enhanced proliferation, migration, and tube formation in endothelial cells. These findings indicate that Adipsin directly enhances angiogenesis by binding with SERBP1, thereby obstructing the interaction of SERBP1 with *SERPINE1* mRNA.

Despite the promising findings, certain limitations need to be acknowledged. First of all, the mouse model of HLI is an acute event in our study that failed to recapitulate the real-world lower extremity PAD. The present study focused on short-term outcomes following HLI and may not fully capture the long-term impacts or potential off-target effects of Adipsin overexpression. Therefore, chronic PAD models should be considered, and clinical patient data need to be integrated in future research to validate these findings. Secondly, the present study exclusively employed HUVECs for mechanistic studies, whereas new vessel formation following femoral artery ligation is predominantly driven by the microvasculature and arterial endothelial cells. Additional cell models should be employed for mechanistic studies to further verify the findings of the current study.

Conclusions

In conclusion, the present study provides clear evidence that Adipsin plays a positive regulatory role in response to HLI in diabetic mice. Adipsin binds to SERBP1 in endothelial cells, disrupting the interaction between SERBP1 and *SERPINE1* mRNA. This disruption decreases the stability of *SERPINE1* mRNA, reduces SERPINE1 expression, and promotes VEGF-induced activation of VEGFR2 (Fig. 8). As

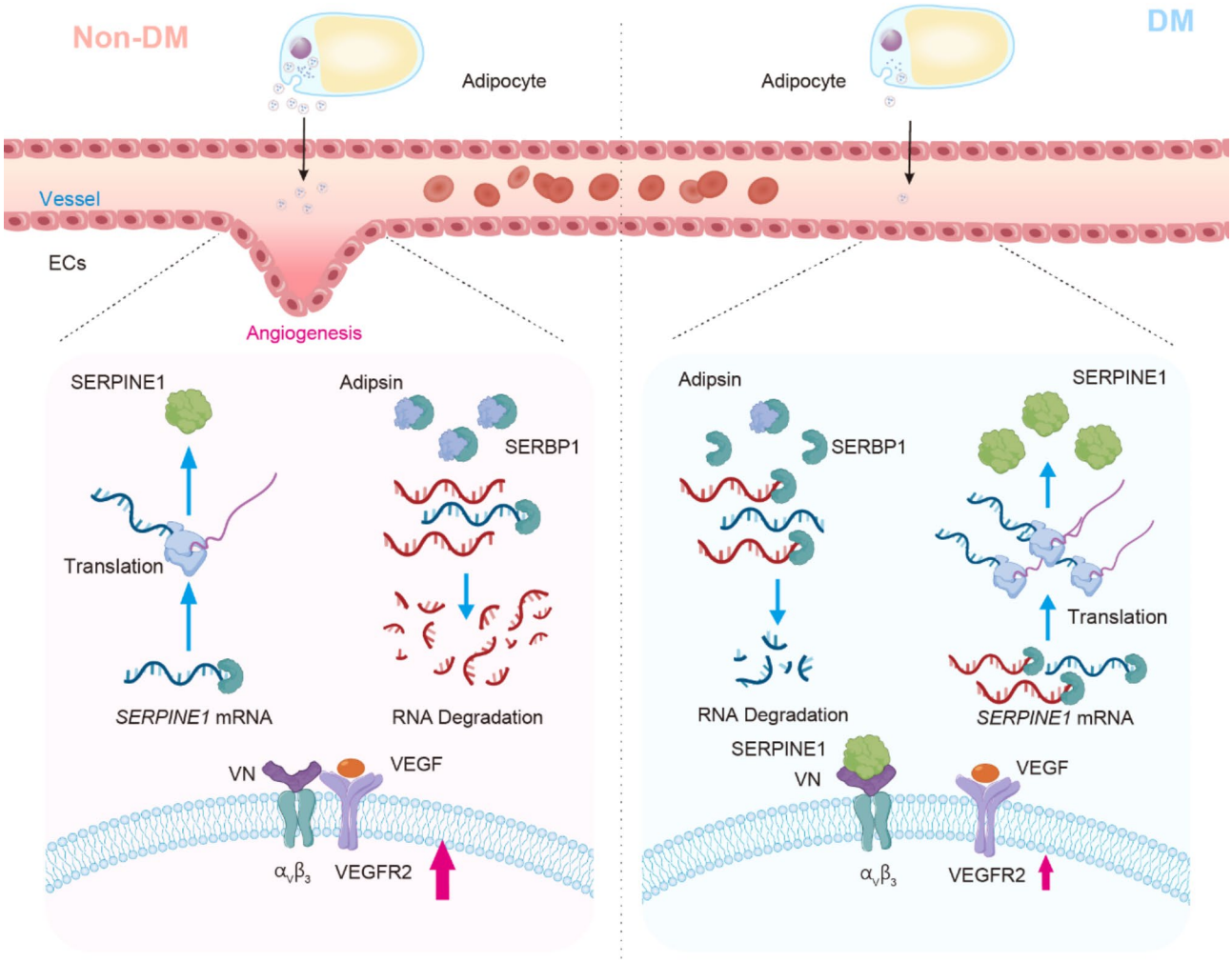

Fig. 8 Graphical illustration of Adipsin-SERPINE1 regulatory mechanism. (1) Adipsin, secreted by adipose tissues, is taken up by endothelial cells. In non-diabetic mice, Adipsin enters endothelial cells and binds to SERBP1, disrupting the interaction between SERBP1 and *SERPINE1* mRNA. This disruption results in decreased stability of *SERPINE1* mRNA, reduced SERPINE1 expression, and enhanced VEGF-induced activation of VEGFR2. Consequently, endothelial cell proliferation and tube formation are increased, promoting angiogenesis. (2) In diabetic mice, the interaction between Adipsin and SERBP1 is diminished due to reduced levels of Adipsin. This leads to increased binding of SERBP1 to *SERPINE1* mRNA, thereby enhancing the stability of *SERPINE1* mRNA and expression of SERPINE1. As a result, SERPINE1 inhibits VEGF-induced activation of VEGFR2, impairing angiogenesis

a result, endothelial cell proliferation and tube formation are increased, which promotes angiogenesis. These findings suggest that targeting Adipsin could be a promising therapeutic strategy for treating PAD.

Abbreviations

CFD	Complement factor D
C3	Complement component 3
HLI	Hindlimb ischemia
GM	Gastrocnemius muscles
T2DM	Type 2 diabetes mellitus
PAD	Peripheral artery disease
Adipsin-Tg	Adipsin tissue-specific transgenic mice
ECs	Endothelial cells
HFD	High-fat diet
ND	Normal diet
HG	High glucose
STZ	Streptozotocin
GTT	Glucose tolerance test
PFA	Paraformaldehyde
PBS	Phosphate-buffered saline
ECM	Endothelial cell medium
FBS	Fetal bovine serum
MOIs	Multiplicities of infection
dpl	day post-ligation
EGFP	Enhanced green fluorescent protein
HUVECs	Human umbilical vein endothelial cells
SMA	Smooth muscle actin
VEGF-A	Vascular endothelial growth factor-A
VEGFR2	Vascular endothelial growth factor receptor 2
TF	Transferrin
SERBP1	SERPINE1 mRNA binding protein 1
PAI-1	Plasminogen activator inhibitor-1
Co-IP	Co-immunoprecipitation
MS	Mass spectrometry

GSEA	Gene set enrichment analysis
WAT	White adipose tissue
MI	Myocardial infarction

Supplementary Information

The online version contains supplementary material available at https://doi.org/10.1186/s12933-024-02526-2.

Supplementary Material 1

Supplementary Material 2

Supplementary Material 3

Supplementary Material 4

Acknowledgements
The authors thank Dan Li from the microscopy core facility for her instructive guidance. We also thank Analysis & Testing Laboratory for Life Sciences and Medicine of Air Force Medical University for laboratory instruments.

Author contributions
DDS conceived the study design and carefully revised the manuscript. XHZ, MYJ, and XBZ made substantial contributions to the study concept and design, data analysis and interpretation, drafting, and revision of the manuscript. YXZ, HLZ and ZTT made substantial contributions to data acquisition, analysis, and interpretation. JL, YZ, XCD, WG, HHQ, CS and FY provided technical support and contributed to the discussion of the manuscript. JYZ, YL and XJY were responsible for animal models and data collection. YYW were responsible for drawing schematics. DDS served as the guarantor of this work, maintaining full access to all data and ensuring the integrity and accuracy of the data analysis. The study received unanimous approval from all authors prior to submission, and all authors have read and approved the final version of this manuscript.

Funding
This work was supported by the National Natural Science Foundation of China (82470358, 82070398, 81922008), Key basic research projects of basic strengthening plan (2022-JCJQ-ZD-095-00), Key logistic research projects (BKJWS221J004), Shaanxi Provincial Science and Technology Innovation Team (2024RS-CXTD-78), Top Young Talents Special Support Program in Shaanxi Province (2020), Xijing Hospital Research Promotion Program (XJZT24CZ13, XJZT24JC36, XJZT24LY38, LHJJ2023-YX05) and Shaanxi Province Key Technology Research Project (2024SF2-GJHX-27).

Availability of data and materials
The datasets generated or analyzed during this study are available from the corresponding author on reasonable request.

Declarations

Ethics approval and consent to participate
All experimental animal procedures were approved by the Animal Care and Use Committee of the Air Force Medical University and followed the Animal Research Advisory Committee of the National Institutes of Health guidelines (Approval ID: 20201017).

Consent for publication
Not applicable.

Competing interests
The authors declare no competing interests.

Received: 10 October 2024 / Accepted: 25 November 2024
Published online: 02 December 2024

References

1. Ahmad E, Lim S, Lamptey R, Webb DR, Davies MJ. Type 2 diabetes. Lancet. 2022;400:1803–20.
2. Li Y, Liu Y, Liu S, Gao M, Wang W, Chen K, et al. Diabetic vascular diseases: molecular mechanisms and therapeutic strategies. Signal Transduct Target Ther. 2023;8:152.
3. Demir S, Nawroth PP, Herzig S, Ekim Üstünel B. Emerging targets in type 2 diabetes and diabetic complications. Adv Sci. 2021;8:2100275.
4. Yang S, Zhu L, Han R, Sun L, Li J, Dou J. Pathophysiology of peripheral arterial disease in diabetes mellitus. J Diabetes. 2017;9:133–40.
5. Marso SP, Hiatt WR. Peripheral arterial disease in patients with diabetes. J Am Coll Cardiol. 2006;47:921–9.
6. Jude EB, Oyibo SO, Chalmers N, Boulton AJ. Peripheral arterial disease in diabetic and nondiabetic patients: a comparison of severity and outcome. Diabetes Care. 2001;24:1433–7.
7. Criqui MH, Aboyans V. Epidemiology of peripheral artery disease. Circ Res. 2015;116:1509–26.
8. Carmeliet P, Jain RK. Molecular mechanisms and clinical applications of angiogenesis. Nature. 2011;473:298–307.
9. Jain RK. Molecular regulation of vessel maturation. Nat Med. 2003;9:685–93.
10. Zhang X, Duan Y, Zhang X, Jiang M, Man W, Zhang Y, et al. Adipsin alleviates cardiac microvascular injury in diabetic cardiomyopathy through Csk-dependent signaling mechanism. BMC Med. 2023;21:197.
11. Martin A, Komada MR, Sane DC. Abnormal angiogenesis in diabetes mellitus. Med Res Rev. 2003;23:117–45.
12. Cook KS, Min HY, Johnson D, Chaplinsky RJ, Flier JS, Hunt CR, et al. Adipsin: a circulating serine protease homolog secreted by adipose tissue and sciatic nerve. Sci (N Y NY). 1987;237:402–5.
13. Xu Y, Ma M, Ippolito GC, Schroeder HW, Carroll MC, Volanakis JE. Complement activation in factor D-deficient mice. Proc Natl Acad Sci USA. 2001;98:14577–82.
14. Cook KS, Min HY, Johnson D, Chaplinsky RJ, Flier JS, Hunt CR, et al. Adipsin: a circulating serine protease homolog secreted by adipose tissue and sciatic nerve. Science. 1987;237:402–5.
15. Lo JC, Ljubicic S, Leibiger B, Kern M, Leibiger IB, Moede T, et al. Adipsin is an adipokine that improves β cell function in diabetes. Cell. 2014;158:41–53.
16. Dahlke K, Wrann CD, Sommerfeld O, Soßdorf M, Recknagel P, Sachse S, et al. Distinct different contributions of the alternative and classical complement activation pathway for the innate host response during sepsis. J Immunol. 2011;186:3066–75.
17. Zwaini Z, Dai H, Stover C, Yang B. Role of complement properdin in renal ischemia-reperfusion injury. CGT. 2018;17:411–23.
18. Gómez-Banoy N, Guseh JS, Li G, Rubio-Navarro A, Chen T, Poirier B, et al. Adipsin preserves beta cells in diabetic mice and associates with protection from type 2 diabetes in humans. Nat Med. 2019;25:1739–47.
19. Jiang M-Y, Man W-R, Zhang X-B, Zhang X-H, Duan Y, Lin J, et al. Adipsin inhibits Irak2 mitochondrial translocation and improves fatty acid β-oxidation to alleviate diabetic cardiomyopathy. Military Med Res. 2023;10:63.
20. Foussard N, Rouault P, Cornuault L, Reynaud A, Buys ES, Chapouly C, et al. Praliciguat promotes ischemic Leg reperfusion in leptin receptor-deficient mice. Circul Res. 2023;132:34–48.
21. Stabile E, Burnett MS, Watkins C, Kinnaird T, Bachis A, la Sala A, et al. Impaired arteriogenic response to acute hindlimb ischemia in CD4-knockout mice. Circulation. 2003;108:205–10.
22. Kim E, Seo SH, Hwang Y, Ryu YC, Kim H, Lee K-M et al. Inhibiting the cytosolic function of CXXC5 accelerates diabetic wound healing by enhancing angiogenesis and skin repair. Exp Mol Med. 2023;1–13.
23. Bao XL, Dai Y, Lu L, Wang XQ, Ding FH, Shen WF, et al. Vasostatin-2 associates with coronary collateral vessel formation in diabetic patients and promotes angiogenesis via angiotensin-converting enzyme 2. Eur Heart J. 2023;44:1732–44.
24. Zhang Y, Cao Y, Zheng R, Xiong Z, Zhu Z, Gao F, et al. Fibroblast-specific activation of Rnd3 protects against cardiac remodeling in diabetic cardiomyopathy via suppression of Notch and TGF-β signaling. Theranostics. 2022;12:7250–66.
25. Simons M. An inside view: VEGF receptor trafficking and signaling. Physiol (Bethesda). 2012;27:213–22.
26. Wang L, Feng Y, Xie X, Wu H, Su XN, Qi J, et al. Neuropilin-1 aggravates liver cirrhosis by promoting angiogenesis via VEGFR2-dependent PI3K/Akt pathway in hepatic sinusoidal endothelial cells. EBioMedicine. 2019;43:525–36.
27. Lee MY, Gamez-Mendez A, Zhang J, Zhuang Z, Vinyard DJ, Kraehling J et al. Endothelial cell autonomous role of Akt1: regulation of vascular

tone and ischemia-induced arteriogenesis. Arterioscler Thromb Vasc Biol. 2018;38:870–9.
28. Praetner M, Zuchtriegel G, Holzer M, Uhl B, Schaubächer J, Mittmann L, et al. Plasminogen activator Inhibitor-1 promotes neutrophil infiltration and tissue injury on ischemia–reperfusion. ATVB. 2018;38:829–42.
29. Wu J, Strawn TL, Luo M, Wang L, Li R, Ren M, et al. Plasminogen activator inhibitor-1 inhibits angiogenic signaling by uncoupling vascular endothelial growth factor receptor-2-αVβ3 integrin cross talk. Arterioscler Thromb Vasc Biol. 2015;35:111–20.
30. Heaton JH, Dlakic WM, Dlakic M, Gelehrter TD. Identification and cDNA cloning of a novel RNA-binding protein that interacts with the cyclic nucleotide-responsive sequence in the Type-1 plasminogen activator inhibitor mRNA. J Biol Chem. 2001;276:3341–7.
31. Criqui MH, Matsushita K, Aboyans V, Hess CN, Hicks CW, Kwan TW, et al. Lower extremity peripheral artery disease: contemporary epidemiology, management gaps, and future directions: a scientific statement from the American Heart Association. Circulation. 2021;144:e171–91.
32. Weinberg MD, Lau JF, Rosenfield K, Olin JW. Peripheral artery disease. Part 2: medical and endovascular treatment. Nat Rev Cardiol. 2011;8:429–41.
33. Inampudi C, Akintoye E, Ando T, Briasoulis A. Angiogenesis in peripheral arterial disease. Curr Opin Pharmacol. 2018;39:60–7.
34. Boucher JM, Bautch VL. Antiangiogenic VEGF-A in peripheral artery disease. Nat Med. 2014;20:1383–5.
35. Stewart DJ, Kutryk MJ, Fitchett D, Freeman M, Camack N, Su Y, et al. VEGF gene therapy fails to improve perfusion of ischemic myocardium in patients with advanced coronary disease: results of the Northern trial. Mol Ther. 2009;17:1109–15.
36. Stahl GL, Xu Y, Hao L, Miller M, Buras JA, Fung M, et al. Role for the alternative complement pathway in ischemia/reperfusion injury. Am J Pathol. 2003;162:449–55.
37. Man W, Song X, Xiong Z, Gu J, Lin J, Gu X, et al. Exosomes derived from pericardial adipose tissues attenuate cardiac remodeling following myocardial infarction by adipsin-regulated iron homeostasis. Front Cardiovasc Med. 2022;9:1003282.
38. Flier JS, Cook KS, Usher P, Spiegelman BM. Severely impaired Adipsin expression in genetic and acquired obesity. Science. 1987;237:405–8.
39. Dimmeler S, Zeiher AM. Akt takes center stage in angiogenesis signaling. Circul Res. 2000;86:4–5.
40. Zhang C, He H, Dai J, Li Y, He J, Yang W, et al. KANK4 promotes arteriogenesis by potentiating VEGFR2 signaling in a TALIN-1–dependent manner. ATVB. 2022;42:772–88.
41. Midkine controls arteriogenesis by. Regulating the bioavailability of vascular endothelial growth factor a and the expression of nitric oxide synthase 1 and 3. EBioMedicine. 2018;27:237–46.
42. Tzima E, Irani-Tehrani M, Kiosses WB, Dejana E, Schultz DA, Engelhardt B, et al. A mechanosensory complex that mediates the endothelial cell response to fluid shear stress. Nature. 2005;437:426–31.
43. Zhou C, Kuang Y, Li Q, Duan Y, Liu X, Yue J, et al. Endothelial S1pr2 regulates post-ischemic angiogenesis via AKT/eNOS signaling pathway. Theranostics. 2022;12:5172–88.
44. Rahman FA, Krause MP. PAI-1, the plasminogen system, and skeletal muscle. IJMS. 2020;21:7066.
45. Dellas C, Loskutoff DJ. Historical analysis of PAI-1 from its discovery to its potential role in cell motility and disease. Thromb Haemost. 2005;93:631–40.
46. Pannacciulli N, de Mitrio V, Marino R, Giorgino R, de Pergola G. Effect of glucose tolerance status on PAI-1 plasma levels in overweight and obese subjects. Obes Res. 2002;10:717–25.
47. Altalhi R, Pechlivani N, Ajjan RA. PAI-1 in diabetes: pathophysiology and role as a therapeutic target. IJMS. 2021;22:3170.
48. Xu Z, Castellino FJ, Ploplis VA. Plasminogen activator inhibitor-1 (PAI-1) is cardioprotective in mice by maintaining microvascular integrity and cardiac architecture. Blood. 2010;115:2038–47.
49. Stefansson S, Petitclerc E, Wong MKK, McMahon GA, Brooks PC, Lawrence DA. Inhibition of angiogenesis in vivo by plasminogen activator Inhibitor-1. J Biol Chem. 2001;276:8135–41.
50. Chan S-L, Bishop N, Li Z, Cipolla MJ. Inhibition of PAI (plasminogen activator Inhibitor)-1 improves brain collateral perfusion and Injury after acute ischemic stroke in aged hypertensive rats. Stroke. 2018;49:1969–76.
51. Tashiro Y, Nishida C, Sato-Kusubata K, Ohki-Koizumi M, Ishihara M, Sato A, et al. Inhibition of PAI-1 induces neutrophil-driven neoangiogenesis and promotes tissue regeneration via production of angiocrine factors in mice. Blood. 2012;119:6382–93.
52. Stefansson S, Lawrence DA. The serpin PAI-1 inhibits cell migration by blocking integrin αvβ3 binding to vitronectin. Nature. 1996;383:441–3.
53. Yuan Y, Zhou D, Chen F, Yang Z, Gu W, Zhang K. SIX5-activated LINC01468 promotes lung adenocarcinoma progression by recruiting SERBP1 to regulate SERPINE1 mRNA stability and recruiting USP5 to facilitate PAI1 protein deubiquitylation. Cell Death Dis. 2022;13:1–13.
54. Shilenok I, Kobzeva K, Stetskaya T, Freidin M, Soldatova M, Deykin A, et al. SERPINE1 mRNA binding protein 1 is associated with ischemic stroke risk: a comprehensive molecular–genetic and bioinformatics analysis of SERBP1 SNPs. IJMS. 2023;24:8716.

Publisher's note